ROLE OF EPIDERMAL GROWTH FACTOR RECEPTOR ON CARDIAC FUNCTION

Yuying Xie

A dissertation submitted to the faculty of the University of North Carolina at Chapel Hill in partial fulfillment of the requirements for the degree of Doctor of Philosophy in the Curriculum of Genetics and Molecular Biology in the School of Medicine.

Chapel Hill
2015

Approved by:

David Threadgill

Fernando Pardo-Manuel de Villena

Tim Wiltshire

Wei Wang

Wei Sun

ABSTRACT

YUYING XIE: Role of Epidermal Growth Factor Receptor on Cardiac Function
(Under the direction of David Threadgill)

The epidermal growth factor receptor (EGFR/ERBB1) was the first discovered member of the ERBB family of tyrosine kinas receptors that includes ERBB2, ERBB3 and ERBB4. After binding by EGF-related ligands, EGFR is activated to induce homodimerization or heterodimerization with other ERBB receptors, resulting in tyrosine kinase activity. Subsequently, autophosphorylation or transphosphorylation of tyrosine residues in the C-terminal tail of the receptor allows the binding of adaptor proteins to trigger intracellular signaling cascades that can lead to proliferation, survival, and anti-apoptosis. As EGFR is expressed in the majority of developing and adult tissues including heart, dysfunction of EGFR activity can cause severe damage in different tissues and even initiate cancers. Several anti-EGFR drugs are already available in the clinic for late stage cancer patients with activated EGFR activity. However, in cancer therapy using anti-ERBB2 drugs, severe cardiotoxicity among patients has been reported, emphasizing the importance of ERBB signaling in cardiac homeostasis. Also with the increases in life expectancy of patients, some types of cancers tend to be treated as a chronic disease. Therefore it is importance to understanding possible cardiac toxicity under chronic suppression of EGFR pathway.

We propose the use of conditional knockout mice lacking EGFR activity in cardiomyocytes to understand the role of EGFR signaling in normal cardiac function. We

demonstrated that chronic repression of EGFR pathway would cause severe cardiac dysfunction with chamber dilations, left ventricular wall thinning and depressed cardiac function.

Left ventricular hypertrophy (LVH) is associated with many cardiovascular diseases and is a risk factor for cardiac related morbidity and mortality. Mice homozygous with EGFR hypomorphic mutation display various background dependent phenotypes including left ventricle hypertrophy. Using two different strains, we mapped a quantitative trait locus (QTL) associated with cardiac hypertrophy. These studies should be useful in understanding the development of LVH and in predicting patients susceptible to cardiatoxicity induced by chronic use of anti-EGFR drugs.

To my deceased grandmother Ms. Chunying Huang
To my parents Ms. Chanyang Feng and Mr. Shengbao Xie
To my wife Dr. Yangfan (Phoebe) Liu and my son Dongchen Terence Xie

ACKNOWLEDGEMENTS

I would never have been able to complete this work without the guidance of my committee members, courage from friends, and support from my wife. I would not be here at the University of North Carolina at Chapel Hill if it was not for my grandma, Chunying Huang, who had spent an enormous of effort and patient to educate me and protect me in the earliest stage of my life.

First of all, I would like to express my deepest gratitude to my mentor, Dr. David Threadgill for supporting me during the past five years. David is someone you will never forget when you ever meet him. He is the most supportive advisor and one of the smartest person I know. He taught me how to pick important problems and provided me an extraordinary amount of freedom to create my own research agenda. During the hard day of my research, he was always optimistic and spent a huge amount of time and effort to guide me through the dark. After my training in Threadgill's Lab, I become not only a better scientist but also a better person.

I am very grateful to my brilliant and helpful committee members. Dr. Fernando Pardo-Manuel de Villena first impressed me by his ability to go through sixty pages slide within 40 min, and later by his extraordinary scientific thought. His advices drove my project to a higher level. Dr. Tim Wiltshire is an expert in QTL mapping. He asked insightful and critical questions to make sure my work is solid. Dr. Wei Sun is the only junior faculty in my committee. Although he had a very busy schedule, when I had any statistics question he is always there to provide helpful advices. I also gratefully thank Dr. Wei Wang for using her precious times to read this thesis and give her critical comments on this thesis.

TABLE OF CONTENTS

LIST OF TABLES

LIST OF FIGURES

LIST OF ABBREVATIONS AND SYMBOLS

Actb   beta-actin

ADAM12   a disintegrin and metalloproteinase domain 12

Adam19   a disintegrin and metalloproteinase domain 19

ANG-II   angiotensin II

AR   Amphiregulin

AREG   amphiregulin

AS   aortic stenosis

ATP   adenosine triphosphate

AV   atrial ventricular

Bax   BCL2-associated X protein

BTC   beta-cellulin

BW   body weight

cAMP   cyclic adenosine monophosphate

Cdh5   vascular endothelial cadherin

cDNA	Complementary DNA
CK	creatine kinase
DCM	dilated cardiomyopathy
E7.0	embryonic day 7.0
EGF	epidermal growth factor
EGFR	epidermal growth factor receptor
Egfr CKO	*Egfr* conditional knockout
$Egfr^{wa2}/^{wa2}$	homozygous *Egfr mutant mice*
$Egfr^{wt}$ %	= 1- recombination efficiency
$Egfr^{\Delta}$	*Egfr* with deletion
EH	essential hypertension
EMT	epithelial-to-mesenchymal transition
EPG	epigen
EREG	epiregulin
ERK1	Extracellular signal-regulated kinase 1
ERK2	Extracellular signal-regulated kinase 2

ET-1   endotelin-1

FS%   fractional shortening percent

Gapdh   Glyceraldehyde 3-phosphate dehydrogenase

GPCR   G-protein coupled receptor

HB-EGF   heparin-binding EGF-like growth factor

HCM   human leukocyte antigen

$hEGFR^{KI/KI}$ homozygous human EGFR knockin mice

HER2   ErbB-2

HLA   human leukocyte antigen

HW   heart weight

HW/BW   heart-to-body weigh ratio

IF   intermale fighting

Kirrel3   kin of IRRE like 3

KO   knockout

LAMP-2   lysosome-associated membrane protein2

LDH	lactate dehydrogenase
LOD	logarithm (base 10) of odds
LV	left ventricule
LVH	left ventricular hypertrophy
LVID,d	left ventricular internal dimension, diastole
LVID,s	left ventricular internal dimension, systole
LVPW,d	left ventricular posterior wall, diastole
LVPW,s	left ventricular posterior wall, systole
mAbs	monoclonal antibodies
M-mode	motion mode
MPD	mouse phenome database
MT	masson's trichrome
Mybpc	myosin binding protein-C
MYBPC3	cardiac myosin-binding protein C
MYH7	β-cardiac myosin heavy chain

Nppa	atrial nautriuretic peptide
Nppb	brain nautriuretic peptide
NRG1	neuregulin 1
NRG2	neuregulin 2
NRG3	neuregulin 3
NRG4	neuregulin 4
p	*p* value
PAF	platelet-activating factor
PAS-H	periodic acid-schiff counterstained with hematoxylin
PBS	Phosphate buffered saline
PE	phenylephrine
PI3K	phosphatidylinositol 3-kinase
PRKAG2	γ-2-regulatory subunit of AMP-activated protein kinase
PTB	phosphotyrosine binding domain
Q1	quantitative trait locus 1

Q2	quantitative trait locus 2
QTL	quantitative trait locus
R26R	Rosa26 reporter
RCE	restraint and cold (4˚C) exposure
RT-PCR	reverse transcription polymerase chain reaction
SEM	standard error of the mean
SH2	Src Homology 2 domain
SNP	single-nucleotide polymorphism
St3gal4	ST3 beta-galactoside alpha-2,3-sialyltransferase 4
STD	standard deviation
TAC	transverse aortic constriction
Tace	TNF-alpha converting enzyme
TGFA or TGF-α	transforming growth factor-α
TK	tyrosine kinase
TKI	tyrosin kinase inhibitor

TNNI3   cardiac troponin I

TNNT2   cardiac troponin T

Tnt   troponin-T

TPM1   α-tropomyosin

TUNEL   Terminal deoxynucleotidyl transferase mediated dUTP Nick End Labeling
                 assay

wa2   waved-2 mutation

Chapter I: ROLE OF ERBB SIGNALING IN CARDIAC DEVELOPMENT AND HOMESTASIS

I.1   Introduction to cardiomyopathy

Cardiomyopathies, diseases of the myocardial tissue, are strongly linked to cardiac dysfunction.[1] In early stages, cardiomypothies may be asymptomatic but as disease progresses typical heart failure-like symptoms present, such as shortness of breath, orthopnea, paroxysmal nocturnal dyspnea and edema. More importantly, cardiomyopathies are often high risk signs for arrhythmia or sudden cardiac death.[1]

The four major types of cardiomyopathies are dilated cardiomyopathy, hypertrophic cardiomyopathy, restrictive cardiomyopathy, and arrhythmogenic right ventricular cardiomyopathy. The cause for cardiomyopathy is still unclear. The possible etiologies include hypertension, coronary artery disease, metabolic disorders, nutritional deficiencies, heart tissue damage, viral myocarditis, chronic rapid heart rate, use of cocaine, pregnancy and genetic defects.[2](Table 1-1)

I.1.1   Dilated cardiomyopathy

Dilated cardiomyopathy (DCM), the most common form of non-ischemic cardiomyopathy, is a condition in which the heart is weakened and dialed and cannot efficiently pump blood. Following coronary artery disease and hypertension, DCM is the third leading cause of heart failure in the United States.[2] The lungs, liver, and other organ systems are typically affected by the decreased heart function.

Epidemiology

The estimated incidence of DCM in the United States is five per 100,000 adults and 0.57 per 100,000 children and the incidence has been increasing, most likely due to better diagnostic methods.[3,4] The mortality rates are approximately 25 percent at one year and 50 percent at five years post-diagnosis.[5,6]

Pathological features

Dilatation of both ventricles is the chief pathological feature of DCM. Frequently, mural thrombi present in the left ventricle and occasionally in both atria, which are also usually dilated.[7] Both DCM and left ventricular hypertrophy (LVH) present with electrocardiographic changes (increased voltage) and elevated heart weight. However, the thicknesses of the left ventricular free wall and septum are typically normal or thinner with DCM.[7] In addition, secondary dilatations in mitral and tricuspid annuli are frequently present, and microscopical features show hypertrophy and degeneration of myocyte and interstitial fibrosis with presentation of DCM.[7]

Etiology

The etiology of DCM is multifactorial including (1) familial and genetic factors, (2) viral myocarditis (cytotoxic insults), (3) immune abnormalities, and (4) metabolic, energetic and contractile abnormalities. Approximately 30%-50% of DCM cases have a genetic origin.[8,9] In the past few years, much has been learned about DCM genetics. DCM-associated mutations in many different genes have been reported with autosomal dominant inheritance the most common form of inheritance.[10] So far, mutations in over 20 genes have been reported to cause DCM including cardiac actin, desmin, dystrophin, troponin T, and lamin A/C.[10] The mechanisms causing DCM are very different among the different gene mutations; for example impaired force

generation or force transmission is thought to be the mechanism for sarcomere and cytoskeletal protein genes (actin, troponin C, and troponin T). Additional mechanisms include impaired energy production for mitochondrial mutations, disturbed Ca^{2+} metabolism (phospholamban), impaired stretch sensor machinery (titin, telethonin), and defects in nuclear envelope (lamin A/C and tafazzin) (Fig 1-1).[10] Recently, several groups have found DCM causing mutations linked with troponin T, which is part of the thin filament.[11,12] Other groups have mdeled this mutation in mice to study its effect on muscle fibers. Troponin T mutations result in significantly lower Ca^{2+} sensitivity in force generation in the sarcomere, which would be a possible mechanism for the pathogenesis of DCM. Additionally, *TnT*^{-/-} mice develop severe DCM, which recapitulates the phenotype of patients.[12]

Genetic diseases can be classified as Mendelian diseases (monogenic diseases) or multifactorial diseases.[13] Monogenic diseases are rare and are caused by single gene mutations. Although the gene mutations described above are monogenetic with high penetrance, they only explain DCM in rare familial cases. Multifactorial diseases are more common and complex because they may be due to additive or interactive effects of multiple genes. Genes responsible for multifactorial diseases tend to have low penetrance, and to have interactions with environmental factors. Genetic association studies have identified several low-penetrance polymorphisms (susceptibility genes) contributing to DCM including the G994→T mutation in plasma platelet-activating factor (*PAF*) acetylhydrolase, and a 14-bp deletion polymorphism in human leukocyte antigen (*HLA*).[14-16]

I.1.2 Hypertrophic cardiomyopathy

Hypertrophic cardiomyopathy (HCM), characterized by left and/or right ventricular hypertrophy, is a disease of the cardiac muscle.[1] HCM is usually asymmetric and involves the

interventricular septum.[1] Typically in patients with HCM, the left ventricular volume is normal or reduced and the systolic gradients are normal. HCM is the leading cause of sudden cardiac death in young athletes.[2,17] However, it can occur patients of any age with disabling cardiac symptoms or sudden unexpected cardiac death.

Epidemiology

Hypertrophic cardiomyopathy is likely the most frequently occurring cardiomyopathy with an incidence of 0.2% in the general population, affecting around 600,000 people in the United States.[2] Previous studies have shown that annual mortality for HCM is about 1.4%, and this mortality can be stratified to sudden death (0.7%), progressive heart failure (0.5%) or stroke-related death (0.2%).[18] In young patients sudden death is the major outcome, while progressive heart failure and stroke related death is most common in patients after mid-age.[18] Most patients with HCM have little or no disability and can have normal life expectancy indicating additional factors contribute to sudden death or progressive disease.

Pathological features

Left Ventricular Hypertrophy (LVH) is the most common feature of HCM. However, with the heterogeneity of HCM, no single pattern of LVH is dominant and can include hypertrophy in the LV apex, symmetric hypertrophy and basal septum hypertrophy.[19] There is no direct linkage between the pattern of LV thickening and pathological outcome. At the cellular level, myocardial architecture in LV is frequently disorganized, and myocytes have irregular shapes with multiple intercellular connections.[19] Intramural coronary arteries are also often impaired in HCM, and are characterized by thickened walls with narrowed lumens. As a result, bursts of myocardial ischemia and myocyte death occur, followed by replacement fibrosis.[19] Architectural disorganization and scaring in the myocardium results in unstable

electrophysiological characteristic, ultimately leading to arrhythmias and sudden death in HCM.[20]

Because of the heterogeneity of HCM, the clinical course for individual patients can be classified into one of subgroups: 1) no or mild symptoms, 2) high risk for sudden cardiac death, 3) progressive heart failure with exertional dyspnea and functional disability, and 4) atrial fibrillation often accompanied by embolic stroke.[19] Although sudden death can occur at a wide range of ages, progressive heart failure and stroke occur more frequently in mid-age and older.[21] Risk factors for sudden death include: 1) patients with a prior cardiac arrest or sustained ventricular tachycardia, 2) family history of sudden death due to HCM, 3) syncope or near syncope particularly when it is related to physical activity or when it occurs several times, 4) repeatedly ventricular tachycardia on serial ECG recording, 5) failure of blood pressure to respond to exercise, especially for people younger than 50, and 6) extreme LVH with wall thickness > 30 mm.[19,22] Additional risk factors that have been suggested include atrial fibrillation, myocardial ischemia, alcohol septal ablation surgery, LV outflow obstruction and bridged left anterior descending coronary artery.[19,22]

Etiology

Approximately 50% of hypertrophic cardiomyopathy cases are familial with most inherited as a Mendelian autosomal dominant trait and caused by mutations in one of a number of genes that encode proteins of the cardiac sarcomere (thick or thin filaments).[19,23] Genes responsible for HCM include β–cardiac myosin heavy chain (*MYH7*), cardiac myosi-binding protein C (*MYBPC3*), cardiac troponin T (*TNNT2*), cardiac troponin I(*TNNI3*), and α-tropomyosin (*TPM1*).[24] *MYH7, TNNT2* and *MYBPC3* mutations dominate the familial cases with other genes accounting for a small portion of HCM cases. In addition, two nonsarcomeric

protein mutations, γ-2-regulatory subunit of AMP-activated protein kinase (*PRKAG2*) and

lysosome-associated membrane protein2 (*LAMP-2*) have been linked to HCM.[2] However, the

molecular defects and mechanisms responsible for HCM are usually different in unrelated

patients, and many additional mutations responsible for HCM remain to be identified. Possible

mechanisms for HCM are impaired ATPase activity in cardiomyocytes leading to improper

systolic and diastolic pressures, reduced contractile function leading to hypertrophy in

cardiomyoctes, and disorganized sarcomere structure leading to stimulation of growth factors

which would cause hypertrophy and fibrosis.[25]

In recent years, an increasing number of mouse models have been created to model

human HCM, such as missense mutations in α-MHC gene, transgenic mice expressing a

troponin-T (*Tnt*) missense mutation, and transgenic mice with mutant myosin binding protein-C

(*Mybpc*) lacking binding domains.[26-28]

I.2   Brief outline of heart development

I.2.1   Cardiac development

The heart is the first definitive organ that forms during embryogenesis. At embryonic

day 7.0 (E7.0), cardiac progenitors are located in the primary heart field, a region of mesoderm

that migrates and converges at the midline of the embryo to form the cardiac crescent. (Figure

1.2 a,b)[29] By E8.0, the halves of the cardiac crescent have fused to become a heart tube that

consists of an endothelial tube surrounded by a layer of myocardial cells. (Figure 1.2 c)[29] A

crucial remodeling process known as cardiac looping then starts from E8.5 to E10.5. (Figure 1.2

d-h) During cardiac looping, the tube elongates and adopts a pronounced rightward curvature.

The cardiac tube is then transformed into a heart structure with four distinct chambers through a

series of step including formation of the atrioventricular canal (Figure 1.2 e), formation of the endocardial cushion that will develop to four major heart valves (Figure 1.2 f), and formation of trabeculae within walls of left and right ventricle. (Figure 1.2 g)[29] After spetation of the atria and ventricle and remodeling of the outflow tract, cardiac maturation is complete. The heart is the first definitive organ that forms during embryogenesis. At embryonic day 7.0 (E7.0), cardiac progenitors are located in the primary heart field, a region of mesoderm that migrates and converges at the midline of the embryo to form the cardiac crescent (Figure 1.3 a,b).[29] By E8.0, the halves of the cardiac crescent have fused to become a heart tube that consists of an endothelial tube surrounded by a layer of myocardial cells (Figure 1.3 c).[29] A crucial remodeling process known as cardiac looping then starts from E8.5 to E10.5 (Figure 1.3 d-h). During cardiac looping, the tube elongates and adopts a pronounced rightward curvature. The cardiac tube is then transformed into a heart structure with four distinct chambers through a series of step including formation of the atrioventricular canal (Figure 1.3 e), formation of the endocardial cushion that will develop to four major heart valves (Figure 1.3 f), and formation of trabeculae within walls of left and right ventricle (Figure 1.3 g).[29] After septation of the atria and ventricle and remodeling of the outflow tract, cardiac maturation is complete.

I.2.2 Valve development

There are two steps for cardiac valve formation: cardiac cushion formation and valve remodeling. Following cardiac looping, the extracellular matrix, known as cardiac jelly, expands to form the cardiac cushion in the atrioventricular canal and the distal portion of the outflow tract, which are precursors of tricuspid and mitral valves and the aortic and pulmonic valves, respectively. Before onset of cushion formation, the cardiac jelly is surrounded by the endocardium and myocardium layers. During valve formation, the endocardium undergoes an

7

epithelial-to-mesenchymal transition (EMT) following activation from adjacent myocardium.[29]

This transition involves down-regulation of the cell-adhesion molecule vascular endothelial

cadherin (*Cdh5*), which enables a subset of endocardial cells to delaminate and invade the

cardiac jelly.[29] These cells differentiate to mesenchymal cells and proliferate to form the cardiac

cushions. Endocardial cushion formation is complete by E12.5, and then cushions undergo a

valve remodeling process in which cell proliferation is decreased and apoptosis increased

changing the cushion into a slender valve leaflet by E15.5.

I.3 Role of ERBB family signaling in cardiac development and function

I.3.1 EGFR and ERBB family

The epidermal growth factor receptor (EGFR/ERBB1) was the first discovered member

of the ERBB family of tyrosine kinas receptors that includes ERBB2, ERBB3 and ERBB4.[30]

Members of ERBB family are membrane bound glycoproteins whose basic function is to

transmit extracellular signals into cellular responses. EGFR as well as other members of the

ERBB family have a conserved protein structure containing an extracellular cysteine-rich ligand

binding domain (except for ERBB2/HER2), a single alpha-helix transmembrane domain, an

intracellular tyrosine kinase (TK) domain (except for ERBB3/HER3) and a C-terminal tail with

several tyrosine residues that can serve as docking sites for adaptor proteins after

phosphorylation. The ERBB receptor is activated by binding EGF-related ligands in an

autocrine or paracrine manner, which induce homodimerization or heterodimerization with other

ERBB receptors, resulting in tyrosine kinase activity.[31] Subsequently, autophosphorylation or

transphosphorylation of tyrosine residues in the C-terminal tail allows the binding of adaptor

protein containing SH2 or PTB domains to trigger intracellular signaling cascades. Depending

on the ligand, biological output of signaling cascade can be diverse including proliferation, migration, adhesion, motility and survival.[32] ERBB2 is an orphan receptor with no recognized ligand, while ERBB3 lacks intrinsic kinase activity. Therefore, ERBB2 and ERBB3 can only function through heterodimerization with other ERBB receptors.[33,34]

One of the complexities of ERBB signaling stems from the diversity of ligands. In addition to epidermal growth factor (EGF), there are ten known ligands for ERBB receptors including amphiregulin (AREG), transforming growth factor-α (TGFA), heparin-binding EGF-like growth factor (HB-EGF), betacellulin (BTC), epiregulin (EGEG), epigen (EPG), and neuregulins (NRG 1-NRG4).[35-43] EGF, TGFA, AREG and EREG are specific for EGFR/ERBB1, while HB-EGF, BTC and EPR can activate both EGFR/ERBB1 and ERBB4. (Figure 1.2) NRG1 and NRG2 are ligands for both ERBB3 and ERBB4, but NRG3 and NRG4 have higher preference for ERBB4.[44] After ligand binding, the activated receptors recruit and phosphorylate downstream effecter proteins to activate a cascade of intracellular signaling pathways. The mitogen-activated protein kinase pathway, which is a target of all ERBB receptors, and the phosphatidylinositol 3-kinase (PI3K)-AKT pathway, which are target for a subset of ERBB dimmers, are the most well-studied. The activated receptors are subsequently endocytosed and either degraded in the endosome or recycled to the plasma membrane. Signal termination is an additional control for the biological response of ERBB signaling.

To add another layer of complexity, the ERBB family is also involved in other signaling networks through cross-activation with other receptor classes. For example, members of the G-protein coupled receptor protein (GPCR) family can transactivate EGFR by a so called "triple membranepassing signaling" paradigm, which involve the activation of metalloproteases and subsequent cleavage and release of EGF-like ligands that can bind to EGFR.[45,46] This is the

proposed the mechanism that GPCR agonists, such as angiotensin II(ANG-II) and endotelin-1 (ET-1), triggers cardiomyocyte hypertrophy.[47]

I.3.2   ERBB and ligand knockouts

Evidences from knockouts in genes coding for ERBB receptors and their ligands have suggested the vital role for ERBB signaling in cardiac pathologies (Table 1-2). *Erbb2*, *Erbb4* and *Nrg*1 null mice all die around E10.5 with severe defects in cardiac trabeculae formation.[48-50] Although mice deficient for *Erbb3* have normal cardiac trabeculae, they have defective valve formation resulting embryonic lethal at E13.5.[51,52] *Egfr* null mice show various timing of lethality ranging from pre-implantation to two to three weeks after birth depending on the genetic background.[53-55] Surviving *Egfr* null mice on a mixed CD-1 background exhibit severe semilunar valve enlargement.[48] Compared with the critical role of ERBB receptors on cardiac development, cardiac phenotype in mice lacking ERBB ligands are modest. Mutations in the majority of the ten known ligands including *Egf*, *Areg*, *Tgfa*, *Btc*, *Ereg* and *Nrg-2* show no cardiovascular defects indicating that there is considerable redundancy or functional overlap in the action of specific ligands.[44] However, genetic ablation of *Hb-egf* exhibits severe defects in heart chamber and valve formation.[56] Moreover, *Nrg-1* null mice also have cardiac traveculae defect.[50] In sum, *Erbb* and ligand knock-out models suggest distinct roles for ERBB receptors and ligands during cardiovascular development with ERBB2, ERBB4 and NRG1 signaling being involved in trabeculae formiation, while HB-EGF and EGFR being central to cardiac valve development.

I.3.3   ERBB signaling in cardiac development

ERBB signaling is required for the mid to late gestational cardiac development, specifically for the cardiac trabeculae formation and valve development. Trabeculae and valve

formation both require reciprocal signaling between endocardium and myocardium to regulate cell proliferation, differentiation, and cell invasion to cardiac jelly. In wild-type mice, between E9.5 to 10.5, the expression of ERBB2 and ERRB4 are restricted to cardiac myocardial cells, and NRG-1 is specifically expressed in endocardial cells. From gene targeting studies, mice lacking *Erbb2*, *Erbb4 and Nrg1* all die around E10.5 due to the trabeculae defects that develop into arrhythmia, enlarged ventricule, and reduced blood flow.[48-50] Moreover, other studies have shown expression of ERBB2 and ERBB4 under the control of cardiac specific promoters in *Erbb2* and *Erbb4* null mice, respectively, can rescue the trabeculae defects.[57,58] Because *Egfr* and *Erbb3* null mice show no trabecular defects and neither *Erbb2* nor *Erbb4* can compensate for the loss of the other, cardiac trabeculae formation seems to require NRG-1 signaling through ERBB2/ERBB4 heterodimers.

While ERBB2 and ERBB4 are particularly important in trabeculation, ERBB3 and EGFR have vital roles in cardiac valve formation. During cardiac development, the expression of ERBB3 is restricted to endocardial cushion mesenchyme, and *Erbb3* null mice die at E13.5 due to defective cardiac cushions completely lacking mesenchymal cells.[50,51] Although ERBB3 lacks tyrosine kinase activity, NRG-1 can induce the heterodimerization between ERBB2 and ERBB3, which can trigger downstream signaling by the tyrosine kinase activity on ERBB2. Moreover, close inspection of endocardial cushions in *Erbb2* and *Nrg-1* null embryos shows underdeveloped cushion at E10.5.[48,50] This result suggests that NRG-1 signaling to–ERBB2/ERBB3 heterodimers is required at the early stages of cellular proliferation and differentiation in endocardial cushion formation.

At E14.5, the expression of EGFR is detectable throughout the heart, but enriched in the endocardial cushion.[59] EGFR signaling is particularly important in valve remodeling process,

which is a later stage during valve formation. Mice homozygous for the *Egfr* hypomorphic

waved-2 mutation (*Egfr*[wa2/wa2]) have enlarged aortic and pulmonic valves, and another study

using *Egfr* null mice showsed hyperplastic semilunar (aortic and pulmonic) and AV (mitral and

tricuspid) valves.[48,59] The role of EGFR signaling during cardiac development is also observed

in zebrafish.[60] Addition of an EGFR kinase inhibitor or the transient knockdown of EGFR

expression also results in decreased circulation and a narrowed outflow tract suggesting that

EGFR signaling function in cardiac development is conserved across species.[56,59,60] Consistent

with valve defects in *Egfr* null mice, mice lacking its ligand *Hb-egf* or the convertases *Tace*

(TNF-alpha converting enzyme) or *Adam19* (a disintengrin and metalloproteinase domain 19)

also show cardiac valve abnormalities in semilunar and AV valve.[59,61] During embryonic heart

valve development the expression of HB-EGF is restricted exclusively to endocardial cells, and

is not detected in differentiated mesenchymal cells.[59] Analysis of *Hb-egf* null mice suggests that

HB-EGF-EGFR signaling might regulate valve remodeling rather than cushion formation

because 1) EMT is normal in *Hb-egf* null mice, 2) there is no change in apoptosis rate in *Hb-egf*

null mice, and 3) excessive proliferation of mesenchymal cells is detected in *Hb-egf* null mice.[59]

Available data suggests a paracrine model for EGFR signaling in valve formation where HB-

EGF is released from the plasma membrane of the endocardial cells and diffuses to activate

EGFR on mesenchymal cells to activate downstream signals that suppresses mesenchymal cell

proliferation.

I.3.4 ERBB signaling in maintenance of mature heart function

As in the developing heart, ERBB signaling is particularly important to maintain

homeostasis in the mature heart. Although expression of ERBB receptors declines after

midembryogenesis, EGFR, ERBB2 and ERBB4 are present in postnatal myocardium, with

ERBB4 as the most prevalent receptor.[48] *In vitro* studies have provided evidence that NRG-1, ERBB2, and ERBB4 are implicated in both hypertrophic and survival signaling pathways in adult cardiomyocyte.[48] Several clinical studies suggest an association between heart failure and decreased ERBB2 and ERBB4 protein level.[62,63] Consistent with these clinical finding, ERBB2 and ERBB4 expression is upregulated in heart failure patients whose cardiac function was improving after mechanical ventricular unloading.[62] Moreover, downregulation of ERBB2 activity by using anti-breast cancer drug Trastuzmab, a humanized monoclonal antibody designed to block ERBB2's ligand binding site, resulted in cardiac dysfunction in some patients.[64,65] These findings were recapitulated in *Erbb2*-deficient conditional mutant mice (*Erbb2* CKO mice) which develop severe heart failure with dilated ventricles and decreased contractility by three months of age. [48,66] *Erbb4* conditional knock-out mice with 80% reduction in ventricular ERBB4 protein levels also develop a cardiac phenotype similar to *Erbb2* CKO mice, suggesting that ERBB2 may partner with ERBB4 to form a heterodimer required for maintenance of normal cardiac function.[67]

Ligands for ERBB receptors, such as HB-EGF and NRG1, have also been shown to play important role in postnatal heart. Adult cardiomyocyte strongly express HB-EGF, and the constitutive tyrosine phosphorylation levels of ERBB2 and ERBB4 are significantly reduce in cardiomyocyte from *HB-EGF* knock out mice.[44] These mice also developed a dilated heart with enlarged cardiomyocytes and depressed cardiac function. Moreover, in mice with hypertrophy induced by pressure overload or GPCR agonists, inhibition of HB-EGF shedding by adding DAM12 inhibitor attenuated hypertrophic changes and improved cardiac function.[68]

Compared to wild-type mice, mice lacking one copy of *Nrg1* had more severe cardiotoxicity after exposure to doxorubicin, a chemotherapeutic agent known to cause

cardiomyocyte death.[69] In this model, the protein level of phosphorylated ERBB2, AKT and ERK1/2 are significantly reduced in *Nrg1*^{+/-} compared with wild-type control indicating the involvement of survival pathway.[69] Consistent with data above, short term intravenous administration of NRG1 improved cardiac performance in ischemic, drug-induced cardiomyopathy, myocaritis and chronic rapid pacing model in rodent and canine models.[70] Interestingly, the survival benefit from NRG1 is additive to angiotensin-converting enzyme inhibitor therapy in ischemic models.[70]

Similar as other ERBB members, EGFR signaling also has vital role in maintenance of mature heart function. Exogenous EGF increases contractility and heart rate by elevating cyclic adenosine monophosphate (cAMP) levels in cardiac myocytes.[71] The increase in cAMP occurs through activation of adenylyl cyclase by EGFR-mediated activation of Gs protein.[71] Moreover, *in vitro* studies using isolated cardiomyocytes showed that exposure to HB-EGF or EGF induce hypertrophy.[72] By using a conditional knock-in approach using the human *EGFR* cDNA, homozygous *hEGFR*[KI/KI] mice develop cardiac hypertrophy and semilunar valve abnormalities, a phenotype that is also present in *Egfr*[wa2/wa2].[73] Another study using cardiomyocyte-specific dominant-negative Egfr system to block cardiac EGFR signaling in young mice show dilated cardiomyopathy with increased left ventricular mass and atrial natriuretic factor expression, and decreased cardiac function.[74] Moreover, chronic repression of EGFR signaling using small molecule tyrosin kinase inhibitor (TKI) appears to affect normal cardiac function in female mice.[53] In this model, mice were treated with two different TKIs, irreversible EKB-569 or reversible AG-1478, orally for three months.[53] An increase in left ventricular wall thickness and the numbers of apoptotic cells, and reduced contractility as measured by percent fractional

shortening were observed in female mice.[53] Taken together, these data suggest that EGFR

signaling is required to maintain normal function.

EGFR signaling may protect the heart against stress-induced injury. Using a restraint-

and-cold (4°C)-exposure (RCE) mice model, Miguel Pareja *et al.* found that heart injury

biomarker, including plasma lactate dehydrogenase (LDH) and creatine kinase (CK), were

increased in a time-dependent manner.[75] By contrast, in another common used stress model,

intermale fighting (IF), only LDH activity is raised.[75] One difference between these two models

is that with IF, but not RCE, plasma EGF concentration is strongly elevated. When mice were

exposed to the EGFR inhibitor, AG-1478, immediately before IF, plasma levels of both

biomarkers was increased.[75]

Conversely, injecting *Egf* prior to RCE exposure significantly reduce LAH and CK

activity. Together, this data supports a cardiac-protective role of EGFR signaling on stress-

induced injury.

EGFR signaling also contributes to cardiac hypertrophy induced by activation of the G-

protein-coupled receptor (GPCR) pathway.[76] GPCR agonists, such as phenylephrine (PE),

angiotensin II (AngII) and endothelin-1 (Et-1), are well-know inducer of cardiomyocyte

hypertrophy.[77-79] All of these molecules transactivate EGFR by increasing shedding of HB-EGF

caused by activation of a specific metalloproteinase.[45] Consistent with this model, blocking the

cross-talk between EGFR and GPCR signaling through metalloproteinase or EGFR inhibitor

attenuates hypertrophic phenotype.[47,68]

I.3.5   Genetic modifiers for EGFR signaling

Mice lacking Egfr show various phenotypes depending on the genetic background. [53-55]

For example, *Egfr* null mice on CF-1 background have degeneration of the inner cell mass,

which results in peri-implantation death.[55] Contrastingly, on a CD-1 background, *Egfr* mutant mice can live up to three weeks after birth with abnormalities in skin, kidney and other organs.[53,55] Additionally, mice homozygous for *Egfr^wa2* have abnormalities in aortic valves and development left ventricular hypertrophy, phenotypes that are also dependent on genetic background.[53] *Egfr^wa2/wa2* mice on a C57BL/6J (B6) background have thicker aortic cusps, higher incidence of heart failure, and shorter lifespan compared with *Egfr^wa2/wa2* mice on 129S1/SvImJ background.[53] Taken together, these results suggest that genetic modifiers exist for EGFR signaling.

Table 1.1: Causes of cardiomyopathy. *Adapted from Wexler et.al 2009.*

Primary	Secondary
Genetic	Autoimmune (systemic lupus)
Arrhythmogenic right ventricular cardiomyopathy	Electrolyte imbalance
Hypertrophic cardiomyopathy	Endocrine (diabetes, hypothyroidism)
Mixed (genetic and nongenetic)	Endomyocardial (fibrosis)
Dilated cardiomyopathy	Infiltrative (amyloidosis, Gaucher disease)
Restrictive cardiomyopathy	Inflammatory (sarcoidosis)
Acquired	Neurologic (neurofibromatosis)
Myocarditis (inflammatory cardiomyopathy)	Nutritional (beriberi)
Peripartum (or postpartum) cardiomyopathy	Radiation
Stress cardiomyopathy	Storage (hemochromatosis)
	Toxic (medications)
	Velocardiofacial syndrome

Figure 1.1: A schematic figure of the dilated cardiomyopathy (DCM) causing mechanism.

Adopt from Kärkkäinen 2007.
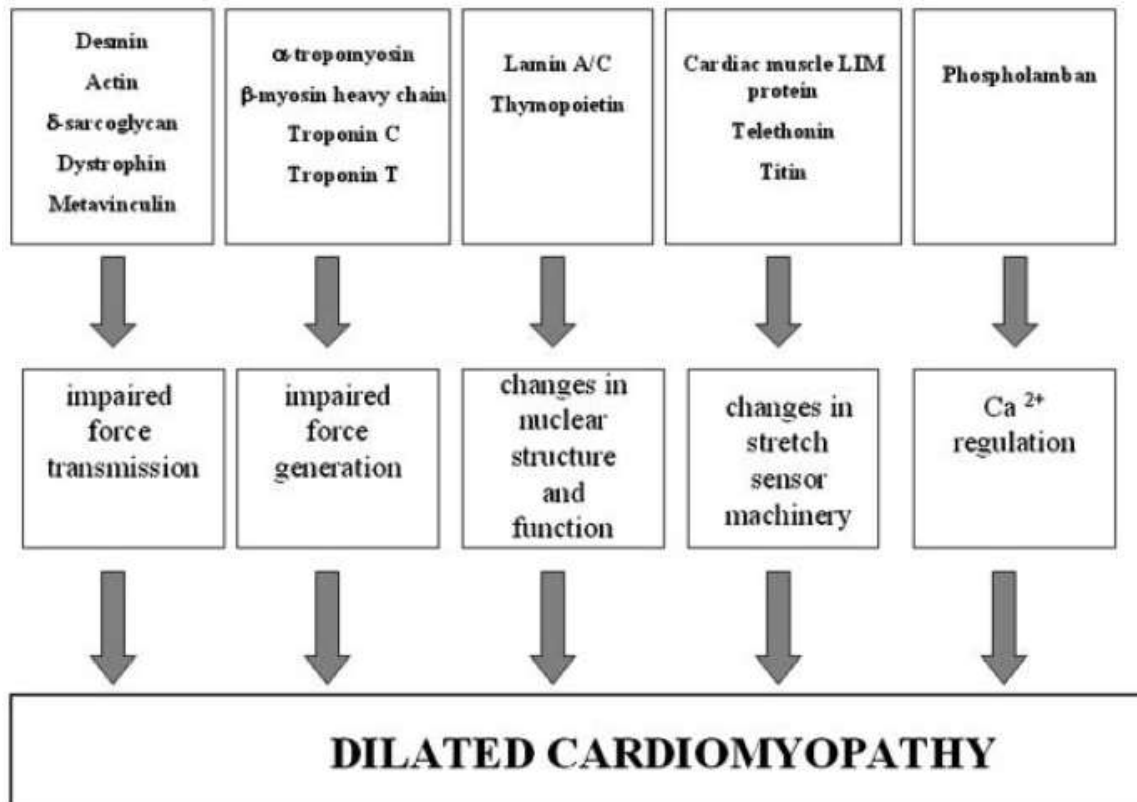
Figure 1.2: The principal stages of cardiac development. *Adapted from Frances et.al 2008.*
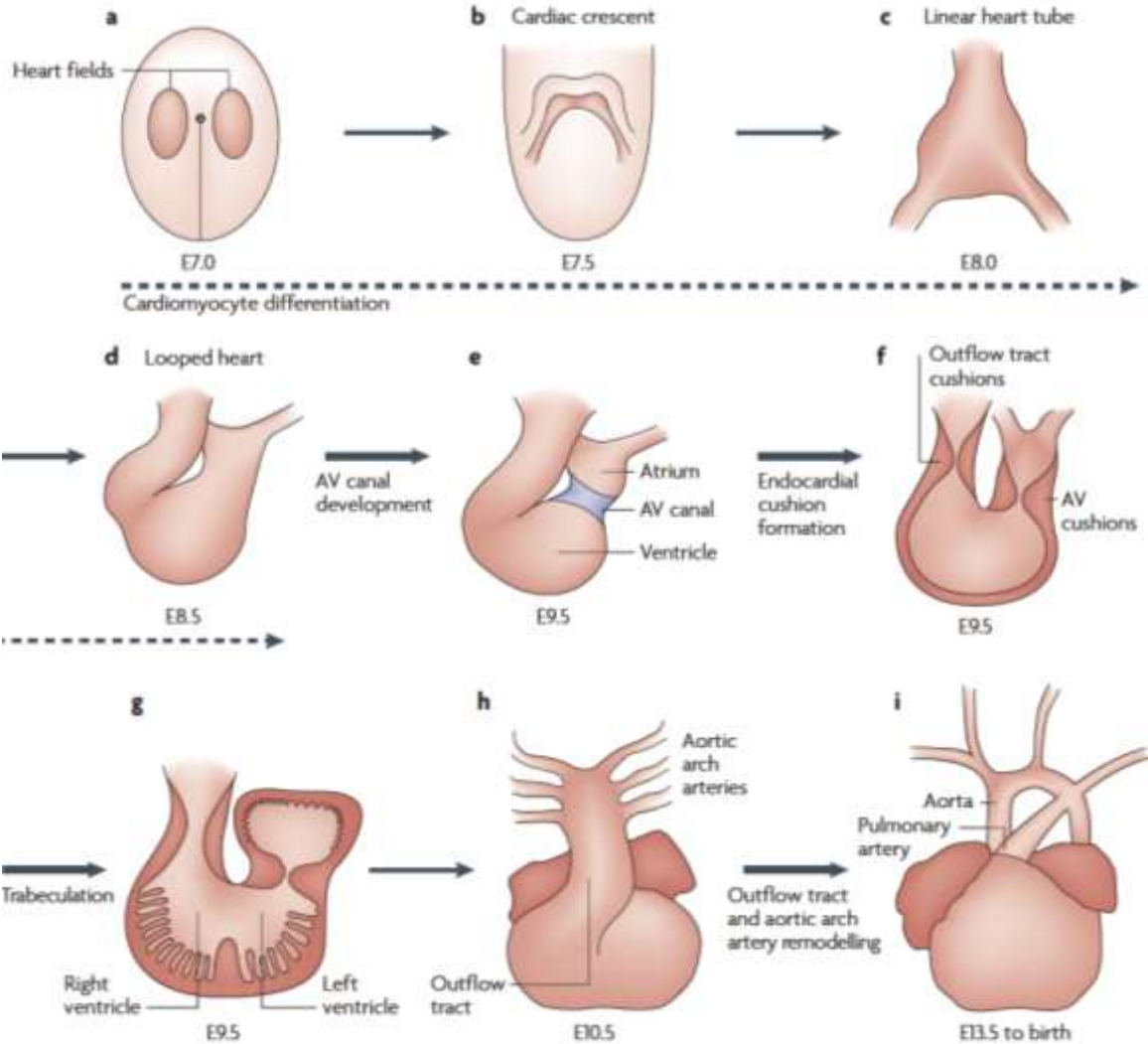
Figure 1.3: Ligand binding specificity for ERBB family. *Adopt from C J Barrick's dissertation.*
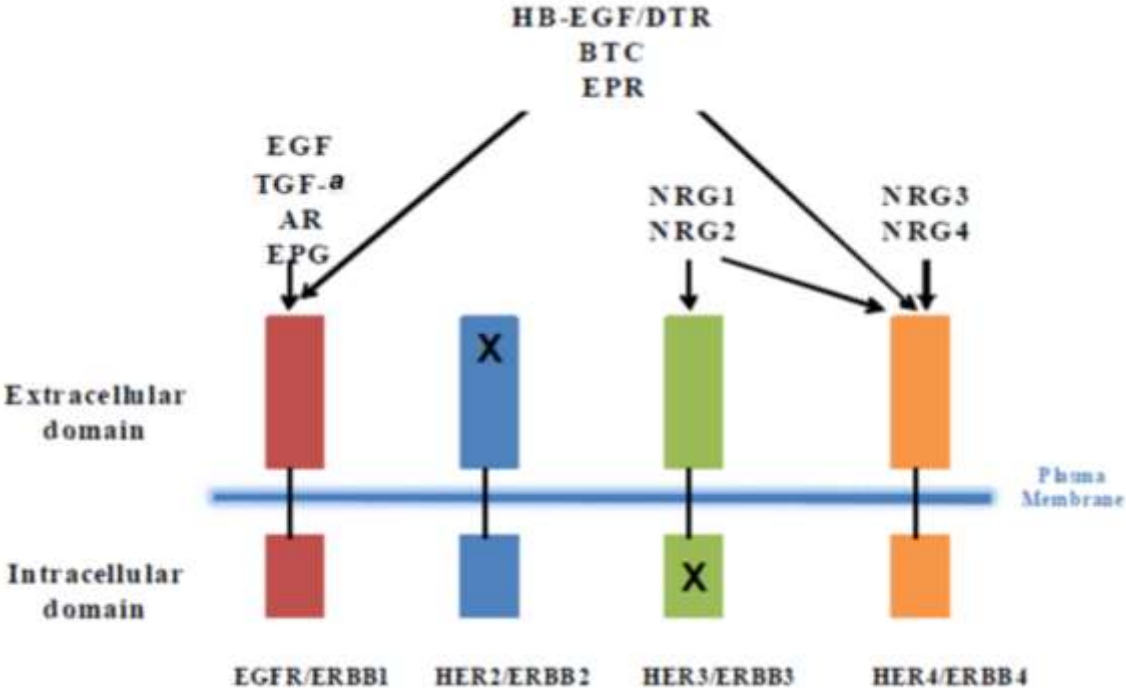
Table 1.2: Phenotype summary from genetic ablation of ERBB receptors, ERBB ligands.

ERBB receptor	Survival	Cardiaovascular system	Other Defects	Reference
ERBB1/EGFR	Embryonic, perinatal or postnatal lethal (genetic background dependent)	Semilunar valve enlargement	-Degeneration of inner cell mass -Defect in placenta, eyelid, skin, lung, kidney, brain, and GI tract	53-55
ERBB2	Embryonic lethal at E10.5	Trabeculae defect	-Nervous system -Mammary gland impaired	48
ERBB3	Embryonic lethal at E13.5	Cushion defect	Nervous system	51,52
ERBB4	Embryonic lethal at E10.5	Trabeculae defect	Mammary gland impaired	49
EGF	Normal	N/A	N/A	83
Amphiregulin (AR)	Normal	N/A	Mammary gland impaired	83
TGF-α	Normal	N/A	Epithelial defect	84
EGF/AR/TGF-α triple	Normal	N/A	-Mammary gland impaired -Defects in small intestine	83,85
HB-EGF	Perinatal or postnatal lethal	Dilated caridac Chamber enlarged valve	Lung, skin, and eyelid	57,60,86
Betacellulin (BTC)	Normal	N/A	N/A	60
BTC/HB-EGF	Perinatal or postnatal lethal	Dilated caridac Chamber enlarged valve	N/A	60
Epiregulin(ER)	Normal	N/A	Dermatitis and immunity defect	87
Neuregulin-1 (NRG1)	Embryonic lethal at E10	Traveculae defect	Nervous system	50
NRG2	Normal	N/A	-Growth retardation -Reduced reproductive capacity	88

REFERENCES

1.   Richardson, P. et al. Report of the 1995 World Health Organization/International Society and Federation of Cardiology Task Force on the Definition and Classification of cardiomyopathies. *Circulation* **93**, 841-2 (1996).

2.   Maron, B.J. et al. Contemporary definitions and classification of the cardiomyopathies: an American Heart Association Scientific Statement from the Council on Clinical Cardiology, Heart Failure and Transplantation Committee; Quality of Care and Outcomes Research and Functional Genomics and Translational Biology Interdisciplinary Working Groups; and Council on Epidemiology and Prevention. *Circulation* **113**, 1807-16 (2006).

3.   Dec, G.W. & Fuster, V. Idiopathic dilated cardiomyopathy. *N Engl J Med* **331**, 1564-75 (1994).

4.   Towbin, J.A. et al. Incidence, causes, and outcomes of dilated cardiomyopathy in children. *Jama* **296**, 1867-76 (2006).

5.   Diaz, R.A., Obasohan, A. & Oakley, C.M. Prediction of outcome in dilated cardiomyopathy. *Br Heart J* **58**, 393-9 (1987).

6.   Fuster, V. et al. The natural history of idiopathic dilated cardiomyopathy. *Am J Cardiol* **47**, 525-31 (1981).

7.   Roberts, W.C., Siegel, R.J. & McManus, B.M. Idiopathic dilated cardiomyopathy: analysis of 152 necropsy patients. *Am J Cardiol* **60**, 1340-55 (1987).

8.   Grunig, E. et al. Frequency and phenotypes of familial dilated cardiomyopathy. *J Am Coll Cardiol* **31**, 186-94 (1998).

9.   Baig, M.K. et al. Familial dilated cardiomyopathy: cardiac abnormalities are common in asymptomatic relatives and may represent early disease. *J Am Coll Cardiol* **31**, 195-201 (1998).

10.   Karkkainen, S. & Peuhkurinen, K. Genetics of dilated cardiomyopathy. *Ann Med* **39**, 91-107 (2007).

11.   Hanson, E.L. et al. Cardiac troponin T lysine 210 deletion in a family with dilated cardiomyopathy. *J Card Fail* **8**, 28-32 (2002).

12.   Kamisago, M. et al. Mutations in sarcomere protein genes as a cause of dilated cardiomyopathy. *N Engl J Med* **343**, 1688-96 (2000).

13.   Colombo, M.G., Botto, N., Vittorini, S., Paradossi, U. & Andreassi, M.G. Clinical utility of genetic tests for inherited hypertrophic and dilated cardiomyopathies. *Cardiovasc Ultrasound* **6**, 62 (2008).

14.   Ichihara, S., Yamada, Y. & Yokota, M. Association of a G994-->T missense mutation in the plasma platelet-activating factor acetylhydrolase gene with genetic susceptibility to nonfamilial dilated cardiomyopathy in Japanese. *Circulation* **98**, 1881-5 (1998).

15.   Lin, A. et al. 14 bp deletion polymorphism in the HLA-G gene is a risk factor for idiopathic dilated cardiomyopathy in a Chinese Han population. *Tissue Antigens* **70**, 427-31 (2007).

16.   Small, K.M., Wagoner, L.E., Levin, A.M., Kardia, S.L. & Liggett, S.B. Synergistic polymorphisms of beta1- and alpha2C-adrenergic receptors and the risk of congestive heart failure. *N Engl J Med* **347**, 1135-42 (2002).

17.   Rosamond, W. et al. Heart disease and stroke statistics--2008 update: a report from the American Heart Association Statistics Committee and Stroke Statistics Subcommittee. *Circulation* **117**, e25-146 (2008).

18.   Maron, B.J. et al. Epidemiology of hypertrophic cardiomyopathy-related death: revisited in a large non-referral-based patient population. *Circulation* **102**, 858-64 (2000).

19.   Maron, B.J. Hypertrophic cardiomyopathy: a systematic review. *Jama* **287**, 1308-20 (2002).

20. Maron, B.J. Contemporary insights and strategies for risk stratification and prevention of sudden death in hypertrophic cardiomyopathy. *Circulation* **121**, 445-56.

21. Kubo, T., Kitaoka, H., Okawa, M., Nishinaga, M. & Doi, Y.L. Hypertrophic cardiomyopathy in the elderly. *Geriatr Gerontol Int* **10**, 9-16.

22. Maron, B.J. Cardiology patient pages. Hypertrophic cardiomyopathy. *Circulation* **106**, 2419-21 (2002).

23. Spirito, P., Seidman, C.E., McKenna, W.J. & Maron, B.J. The management of hypertrophic cardiomyopathy. *N Engl J Med* **336**, 775-85 (1997).

24. Bonne, G., Carrier, L., Richard, P., Hainque, B. & Schwartz, K. Familial hypertrophic cardiomyopathy: from mutations to functional defects. *Circ Res* **83**, 580-93 (1998).

25. Jurynec, J. Hypertrophic cardiomyopathy: a review of etiology and treatment. *J Cardiovasc Nurs* **22**, 65-73; quiz 74-5 (2007).

26. Vikstrom, K.L., Factor, S.M. & Leinwand, L.A. Mice expressing mutant myosin heavy chains are a model for familial hypertrophic cardiomyopathy. *Mol Med* **2**, 556-67 (1996).

27. Tardiff, J.C. et al. Cardiac troponin T mutations result in allele-specific phenotypes in a mouse model for hypertrophic cardiomyopathy. *J Clin Invest* **104**, 469-81 (1999).

28. Yang, Q. et al. In vivo modeling of myosin binding protein C familial hypertrophic cardiomyopathy. *Circ Res* **85**, 841-7 (1999).

29. High, F.A. & Epstein, J.A. The multifaceted role of Notch in cardiac development and disease. *Nat Rev Genet* **9**, 49-61 (2008).

30. Gullick, W.J. Type I growth factor receptors: current status and future work. *Biochem Soc Symp* **63**, 193-8 (1998).

31. Weiss, F.U., Daub, H. & Ullrich, A. Novel mechanisms of RTK signal generation. *Curr Opin Genet Dev* **7**, 80-6 (1997).

32.   Wells, A. EGF receptor. *Int J Biochem Cell Biol* **31**, 637-43 (1999).

33.   Klapper, L.N. et al. The ErbB-2/HER2 oncoprotein of human carcinomas may function solely as a shared coreceptor for multiple stroma-derived growth factors. *Proc Natl Acad Sci U S A* **96**, 4995-5000 (1999).

34.   Horan, T. et al. Binding of Neu differentiation factor with the extracellular domain of Her2 and Her3. *J Biol Chem* **270**, 24604-8 (1995).

35.   Marquardt, H., Hunkapiller, M.W., Hood, L.E. & Todaro, G.J. Rat transforming growth factor type 1: structure and relation to epidermal growth factor. *Science* **223**, 1079-82 (1984).

36.   Ciardiello, F., Dono, R., Kim, N., Persico, M.G. & Salomon, D.S. Expression of cripto, a novel gene of the epidermal growth factor gene family, leads to in vitro transformation of a normal mouse mammary epithelial cell line. *Cancer Res* **51**, 1051-4 (1991).

37.   Ciardiello, F. et al. Differential expression of epidermal growth factor-related proteins in human colorectal tumors. *Proc Natl Acad Sci U S A* **88**, 7792-6 (1991).

38.   Higashiyama, S., Abraham, J.A., Miller, J., Fiddes, J.C. & Klagsbrun, M. A heparin-binding growth factor secreted by macrophage-like cells that is related to EGF. *Science* **251**, 936-9 (1991).

39.   Barnard, J. Betacellulin: newest addition to the epidermal growth factor family. *J Pediatr Gastroenterol Nutr* **17**, 343-4 (1993).

40.   Toyoda, H. et al. Epiregulin. A novel epidermal growth factor with mitogenic activity for rat primary hepatocytes. *J Biol Chem* **270**, 7495-500 (1995).

41.   Kochupurakkal, B.S. et al. Epigen, the last ligand of ErbB receptors, reveals intricate relationships between affinity and mitogenicity. *J Biol Chem* **280**, 8503-12 (2005).

42.   Carraway, K.L., 3rd et al. Neuregulin-2, a new ligand of ErbB3/ErbB4-receptor tyrosine kinases. *Nature* **387**, 512-6 (1997).

43.   Harari, D. et al. Neuregulin-4: a novel growth factor that acts through the ErbB-4 receptor tyrosine kinase. *Oncogene* **18**, 2681-9 (1999).

44.   Iwamoto, R. & Mekada, E. ErbB and HB-EGF signaling in heart development and function. *Cell Struct Funct* **31**, 1-14 (2006).

45.   Prenzel, N. et al. EGF receptor transactivation by G-protein-coupled receptors requires metalloproteinase cleavage of proHB-EGF. *Nature* **402**, 884-8 (1999).

46.   Daub, H., Weiss, F.U., Wallasch, C. & Ullrich, A. Role of transactivation of the EGF receptor in signalling by G-protein-coupled receptors. *Nature* **379**, 557-60 (1996).

47.   Thomas, W.G. et al. Adenoviral-directed expression of the type 1A angiotensin receptor promotes cardiomyocyte hypertrophy via transactivation of the epidermal growth factor receptor. *Circ Res* **90**, 135-42 (2002).

48.   Crone, S.A. et al. ErbB2 is essential in the prevention of dilated cardiomyopathy. *Nat Med* **8**, 459-65 (2002).

49.   Gassmann, M. et al. Aberrant neural and cardiac development in mice lacking the ErbB4 neuregulin receptor. *Nature* **378**, 390-4 (1995).

50.   Meyer, D. & Birchmeier, C. Multiple essential functions of neuregulin in development. *Nature* **378**, 386-90 (1995).

51.   Erickson, S.L. et al. ErbB3 is required for normal cerebellar and cardiac development: a comparison with ErbB2-and heregulin-deficient mice. *Development* **124**, 4999-5011 (1997).

52.   Riethmacher, D. et al. Severe neuropathies in mice with targeted mutations in the ErbB3 receptor. *Nature* **389**, 725-30 (1997).

53. Barrick, C.J., Yu, M., Chao, H.H. & Threadgill, D.W. Chronic pharmacologic inhibition of EGFR leads to cardiac dysfunction in C57BL/6J mice. *Toxicol Appl Pharmacol* **228**, 315-25 (2008).

54. Miettinen, P.J. et al. Epithelial immaturity and multiorgan failure in mice lacking epidermal growth factor receptor. *Nature* **376**, 337-41 (1995).

55. Sibilia, M. & Wagner, E.F. Strain-dependent epithelial defects in mice lacking the EGF receptor. *Science* **269**, 234-8 (1995).

56. Iwamoto, R. et al. Heparin-binding EGF-like growth factor and ErbB signaling is essential for heart function. *Proc Natl Acad Sci U S A* **100**, 3221-6 (2003).

57. Morris, J.K. et al. Rescue of the cardiac defect in ErbB2 mutant mice reveals essential roles of ErbB2 in peripheral nervous system development. *Neuron* **23**, 273-83 (1999).

58. Tidcombe, H. et al. Neural and mammary gland defects in ErbB4 knockout mice genetically rescued from embryonic lethality. *Proc Natl Acad Sci U S A* **100**, 8281-6 (2003).

59. Jackson, L.F. et al. Defective valvulogenesis in HB-EGF and TACE-null mice is associated with aberrant BMP signaling. *Embo J* **22**, 2704-16 (2003).

60. Goishi, K. et al. Inhibition of zebrafish epidermal growth factor receptor activity results in cardiovascular defects. *Mech Dev* **120**, 811-22 (2003).

61. Zhou, B., Rao, L., Peng, Y., Zhang, Q. & Zhang, L. Epidermal growth factor receptor gene polymorphisms, R497K, but not (CA)n repeat, is associated with dilated cardiomyopathy. *Clin Chim Acta* **403**, 184-7 (2009).

62. Uray, I.P. et al. Left ventricular unloading alters receptor tyrosine kinase expression in the failing human heart. *J Heart Lung Transplant* **21**, 771-82 (2002).

63. Rohrbach, S., Niemann, B., Silber, R.E. & Holtz, J. Neuregulin receptors erbB2 and erbB4 in failing human myocardium -- depressed expression and attenuated activation. *Basic Res Cardiol* **100**, 240-9 (2005).

64.   Schneider, J.W., Chang, A.Y. & Rocco, T.P. Cardiotoxicity in signal transduction therapeutics: erbB2 antibodies and the heart. *Semin Oncol* **28**, 18-26 (2001).

65.   Schneider, J.W., Chang, A.Y. & Garratt, A. Trastuzumab cardiotoxicity: Speculations regarding pathophysiology and targets for further study. *Semin Oncol* **29**, 22-8 (2002).

66.   Ozcelik, C. et al. Conditional mutation of the ErbB2 (HER2) receptor in cardiomyocytes leads to dilated cardiomyopathy. *Proc Natl Acad Sci U S A* **99**, 8880-5 (2002).

67.   Garcia-Rivello, H. et al. Dilated cardiomyopathy in Erb-b4-deficient ventricular muscle. *Am J Physiol Heart Circ Physiol* **289**, H1153-60 (2005).

68.   Asakura, M. et al. Cardiac hypertrophy is inhibited by antagonism of ADAM12 processing of HB-EGF: metalloproteinase inhibitors as a new therapy. *Nat Med* **8**, 35-40 (2002).

69.   Liu, F.F. et al. Heterozygous knockout of neuregulin-1 gene in mice exacerbates doxorubicin-induced heart failure. *Am J Physiol Heart Circ Physiol* **289**, H660-6 (2005).

70.   Liu, X. et al. Neuregulin-1/erbB-activation improves cardiac function and survival in models of ischemic, dilated, and viral cardiomyopathy. *J Am Coll Cardiol* **48**, 1438-47 (2006).

71.   Nair, B.G., Rashed, H.M. & Patel, T.B. Epidermal growth factor produces inotropic and chronotropic effects in rat hearts by increasing cyclic AMP accumulation. *Growth Factors* **8**, 41-8 (1993).

72.   Clerk, A., Aggeli, I.K., Stathopoulou, K. & Sugden, P.H. Peptide growth factors signal differentially through protein kinase C to extracellular signal-regulated kinases in neonatal cardiomyocytes. *Cell Signal* **18**, 225-35 (2006).

73.   Sibilia, M. et al. Mice humanised for the EGF receptor display hypomorphic phenotypes in skin, bone and heart. *Development* **130**, 4515-25 (2003).

74. Rajagopalan, V., Zucker, I.H., Jones, J.A., Carlson, M. & Ma, Y.J. Cardiac ErbB-1/ErbB-2 mutant expression in young adult mice leads to cardiac dysfunction. *Am J Physiol Heart Circ Physiol* **295**, H543-54 (2008).

75. Pareja, M., Sanchez, O., Lorita, J., Soley, M. & Ramirez, I. Activated epidermal growth factor receptor (ErbB1) protects the heart against stress-induced injury in mice. *Am J Physiol Regul Integr Comp Physiol* **285**, R455-62 (2003).

76. Saito, Y. & Berk, B.C. Transactivation: a novel signaling pathway from angiotensin II to tyrosine kinase receptors. *J Mol Cell Cardiol* **33**, 3-7 (2001).

77. Simpson, P., McGrath, A. & Savion, S. Myocyte hypertrophy in neonatal rat heart cultures and its regulation by serum and by catecholamines. *Circ Res* **51**, 787-801 (1982).

78. Ito, H. et al. Endothelin-1 induces hypertrophy with enhanced expression of muscle-specific genes in cultured neonatal rat cardiomyocytes. *Circ Res* **69**, 209-15 (1991).

79. Sadoshima, J., Xu, Y., Slayter, H.S. & Izumo, S. Autocrine release of angiotensin II mediates stretch-induced hypertrophy of cardiac myocytes in vitro. *Cell* **75**, 977-84 (1993).

80. Luetteke, N.C. et al. Targeted inactivation of the EGF and amphiregulin genes reveals distinct roles for EGF receptor ligands in mouse mammary gland development. *Development* **126**, 2739-50 (1999).

81. Luetteke, N.C. et al. TGF alpha deficiency results in hair follicle and eye abnormalities in targeted and waved-1 mice. *Cell* **73**, 263-78 (1993).

82. Troyer, K.L. et al. Growth retardation, duodenal lesions, and aberrant ileum architecture in triple null mice lacking EGF, amphiregulin, and TGF-alpha. *Gastroenterology* **121**, 68-78 (2001).

83. Mine, N., Iwamoto, R. & Mekada, E. HB-EGF promotes epithelial cell migration in eyelid development. *Development* **132**, 4317-26 (2005).

84. Britto, J.M. et al. Generation and characterization of neuregulin-2-deficient mice. *Mol Cell Biol* **24**, 8221-6 (2004).

Chapter II: EGFR IS ESSENTIAL IN THE PREVENTION OF DILATED CARDIOMYOPATHY

II.1   Overview

Approximately one third of all human cancer has increased activity in EGFR/ERBB1 signaling, which is associated with poor prognosis. EGFR targeted therapy, which includes monoclonal antibodies (mAbs) and tyrosine kinase inhibitors (TKI), has been widely used on non-small-cell lung cancer, pancreatic cancer, and colorectal cancer, and has improved patient survival significantly. With the improvement in cancer treatment regimen, patients tend to have a longer prognosis, which leads to a prolonged exposure to anti-EGFR drugs. EGFR is known to protect the heart against acute stress, and its ligand, heparin-binding EGF is required to maintain homeostasis of the heart. However, the role of EGFR in a normal heart is not clear. Therefore, the chronic suppression of EGFR signaling from anti-EGFR drugs may lead to unexpected cardiac-toxicity similar to trastuzumab, which is a mAb for ERBB2. To investigate the physiological role of EGFR signaling in the adult heart, we created mice with a cardiomyocyte specific deletion of *Egfr*. These Egfr conditional mutant mice were viable and displayed a normal phenotype. However, physiological analysis revealed a progressively dilated cardiomyopathy, with signs of cardiac dysfunction, generally appearing by the sixth postnatal month. Histological analysis revealed chamber dilations, left ventricular wall thinning and depressed cardiac function in mutant mice. We infer that signaling from the EGFR receptor is crucial for adult heart function. These conditional *Egfr* mutant mice provide a model to assess the possible cardiac side effects from chronic anti-EGFR cancer therapy.

II.2　Introduction

The epidermal growth factor receptor (EGFR/ERBB1) was the first discovered member of the ERBB family of tyrosine kinase receptors that includes ERBB2, ERBB3 and ERBB4.[1] EGFR as well as other members of the ERBB family has a conserved protein structure containing an extracellular cysteine-rich ligand binding domain (except for ERBB2/HER2), a single alpha-helix transmembrane domain, an intracellular tyrosine kinase (TK) domain (except for ERBB3/HER3), and a C-terminal tail with several tyrosine residues that can serve as docking sites for adaptor proteins after phosphorylation.[2] The EGFR receptor is activated by binding EGF-related ligands, which induce homodimerization or heterodimerization with other ERBB receptors, resulting in tyrosine kinase activity.[3] Subsequently, autophosphorylation or transphosphorylation of tyrosine residues in the C-terminal tail allows the binding of adaptor protein to trigger intracellular signaling cascades, including proliferation, survival, and anti-apoptosis.[4]

Mutant EGFR is the main etiology for non-small-cell lung cancer, which accounts for more than 80% of patients.[5] EGFR is also mutated or overexpressed in many other types of tumors including lung cancer, colorectal cancer, and kidney cancer. Tumors with mutant EGFR normally have poor prognosis, including chemotherapy resistance and decreased life-expectancy.[6-8] The dependency of certain cancers on EGFR for maintaining the malignant phenotype is the rationale for molecular targeting EGFR in cancer therapy.[9] To date, several anti-EGFR drugs, such as Gefitinib, Erlotinib, Getuximab and Panitumumab are available in the market for late stage cancer patients with EGFR positive mutation.[10] Those drugs have shown a significant improvement on patient's survival by inhibiting EGFR signaling through blocking

ligand binding (Getuximab and Panitumumab) or competing with adenosine triphosphate (ATP) for binding to kinase pockets (Gefitinib and Erlotinib).[11] With the advance in cancer therapy and the resultant increases in life expectancy among patients, some types of cancers are now treated as a chronic disease. The use of anti-EGFR drugs on a long-term basis emphasizes the importance of knowing the possible cardiac toxicity under chronic suppression of EGFR pathway.

The ERBB signaling pathway is known to be essential for maintaining cardiac homeostasis. The expressions of EGFR, ERBB2 and ERBB4 are all detectable in adult human and rodent hearts. The expression and activation of ERBB2 and ERBB4 are inhibited in failing hearts.[12-14] Moreover, it has been shown that breast cancer therapy using ERBB2 antibody trastuzumab combined with chemotherapy results in unexpected cardiac dysfunction in some patients.[15-17] Mice lacking ERBB2 and ERBB4 in the cardiac ventricles also showed to have dilated cardiomyopathy.[11,18,19] EGFR signaling is involved in promoting cardiachypertrophy through transactivation by the G protein couple receptor (GPCR) pathway.[20,21] Several studies have also shown that ERGF signaling protect the heart against stress-induced injury.[22] Previous studies by our laboratory have shown that mice homozygous for $Egfr^{wa2}$, which is a hypomorphic mutation of $Egfr$, develop cardiac hypotrophy in a C57BL/6J background.[23] However, $Egfr^{wa2}$ mutant mice also develop aortic valve thickening which makes the cardiac dysfunction hard to explain.[23,24] To date, no direct studies have assessed the cardiac effects of chronic suppression of EGFR activity. To address this question, we generated a conditional $Egfr$ knockout (CKO) mouse line through the cardiomyocyte-specific deletion of exon3 using a Cre-loxP system. Mice that were homozygous for the deletion of the $Egfr$ allele were born at the expected Mendelian frequency, and reached adulthood without enlarged aortic valve. However, physiological

analysis revealed a progressive onset of multiple independent parameters of dilated cardiomyopathy. In addition, we found that *Egfr* deficient mice were also more susceptible to stress-induced cardiac dysfunction.

II.3   Materials and Methods

Animals

The generation and genotyping of *Egfr* floxed (*Egfr^{f/f}*) mice and a MHC-cre (*MHC^{cre/+}*) mice have been described.[11,25]   The Rosa26 reporter (R26R) was a gift from Dr. Terry Van Dyke (University of North Carolina at Chapel Hill).

In vivo pressure overload

In vivo pressure overload was induced by transverse aortic constriction (TAC) on 10 *Egfr* conditional knockout (*Egfr* CKO) mice and 6 wildtype littermates with compatible cardiac function, as described previously.[26]   The aorta was constricted between the innominate and left common carotid arteries by tying a silk thread, which produced a stenosis of the vessel. The load produced by TAC was measured using Doppler in the right and left carotid arteries before and after silk ligation. Three mice of *Egfr* CKO and control group received a sham operation in which the aortic arch was isolated but not ligated.

Echocardiography

A two-dimensional long-axis and short-axis views of the left ventricle were obtained using a 30 MHz transducer and the vevo 2100 Ultrasonograph (VisualSonics, Toronto, Canada) in conscious mice. From parasternal long-axis view, an M-mode cursor was positioned to the posterior wall of LV at the level of the papillary muscles. Left ventricular internal dimension, diastole (LVID,d), left ventricular internal dimension, systole (LVID,s), left ventricular posterior

wall, diastole (LVPW,d), left ventricular posterior wall, systole (LVPW,s) were measure from long-axis motion mode (M-mode) tracing. Fractional shortening (FS), a measure of the pumping function of the heart, is calculated by (LVID,d-LVID,s)/LVID,d. All measurement were done from leading edge to leading edge following the American Society of Echocardiography guildlines.[27] Areas of increased velocities in outflow tract are identified by color flow Doppler. Pulsed Doppler was then used to quantify these velocities.

Tissue collection

After mice were weighted, hearts, kidneys and livers were removed from the mice, rinsed in PBS and weighted. Hearts were cut in half at the level of papillary muscle. The top half of heart was fxied in 10% neutral buffered formalin at 4˚C overnight and embedded in paraffin for histological analysis, and the bottom half of heart was snap-frozen for use in cryo-sectioning and RNA extraction.

Histology

The sections were stained with hematoxylin-eosin for examination of gross appearance; while masson's trichrome (MT) or Periodic Acid-Schiff counterstained with hematoxylin (PAS-H) was employed to assess fibrosis, aortic valve size. Cardiomyocyte size was assessed by measuring 100 cardiomyocytes, which are round and have nuclei, per PAS-H stained slide at ten randomly selected fields. To measure the aortic valve size, serial sagittal sections (7 μm) were collected from each heart. Aortic cusp diameter was only measured from sections where the aortic outflow tract and aortic walls were clearly visible and in similar orientation. The value of largest valve in this serial represents the valve size for that individual.

X-gal staining

Cryo-sections of heart samples were fixed with 2% paraformaldehyde on ice for 10 min, and washed in rinse buffer (2 mM MgCl$_2$, 1 X PBS, pH 7.2) for 10 min. Then slides were washed in detergent rinse buffer (2 mM MgCl$_2$, 0.02% Igepal CA 630, 0.01% sodium deoxycholate, 1X PBS, pH 7.2) for 10 min, and followed by incubating in x-gal staining solution for 4 hours at 37 ˚C in a humidified box. Sections were counterstained with hematoxylin and eosin.

Real-Time RT-PCR

Total RNA was extracted from the lower half of the LV using TRIZOL (Invitrogen, Carlsbad, California) according to the manufacturer's protocol. After DNAse treatment, total RNA was reverse transcribed using the High Capacity cDNA Archive Kit (Applied Biosystems, Foster City, California). Taqman primers and probes for mouse Glyceraldehyde 3-phosphate dehydrogenase (*Gapdh*), *Egfr*, atrial nautriuretic peptide (*Nppa*), brain nautriuretic peptide (*Nppb*), BCL2-associated X protein (*Bax*) and beta-actin (*Actb*) were purchased from Applied Biosystem. Real-time quantitative PCR was carried out using Stratagene MX3000P. The threshold count values were normalized to either GAPDH or ACTB.

TUNEL assay

TUNEL was performed using ApopTag Fluorescein *In Situ* apoptosis detection kit (Chemicon) according to the manufacturer's protocol.

Statistical analysis

All data are presented as means±SEM. Statistical analysis was performed with GraphPad Prism (version 5.00 for Windows, GraphPad Software, San Diego, CA). Statistical significance of the difference between two groups was determined using the two-tailed unpaired Student's *t*-

test or nonparametric Mann-Whitney test; while one way ANOVA was used to determine statistical significance between three groups. A p-value of less than 0.05 was considered significant.

II.4   Results

Generation of cardiomyocyte-restricted deletion of *Egfr*

$Egfr^{wa2/wa2}$ and $Egfr$ null mice develop enlarged aortic valves, showing that EGRF signaling is required for normal valve remodeling processes. However, the enlarged valves complicate analysis of associated cardiac phenotypes that subsequently occur.[24] To overcome this limitation, $Egfr$ was deleted exclusively in cardiomyocyte by crossing mice carrying the conditional $Egfr^f$ allele with mice carrying the MHC^{cre} allele, which drives high-efficiency cardiomyocyte specific Cre expression. To assess distribution of Cre expression in $MHC^{cre/+}$ mice, $MHC^{cre/+}$ mice were crossed with $R26R$ mice to obtain $MHC^{cre/+}/R26R$ mice. After staining with x-gal, hearts from $MHC^{cre/+}/R26R$ mice showed β-galactosidase activity in the myocardium, but not in the valves. (Figure 2.1) Although MHC^{cre} introduced recombination of the $Egfr^f$ allele in cardiomyocytes with high efficiency as determined by PCR of left ventricle DNA, some non-recombined $Egfr^f$ alleles remained in the left ventricle resulting in mosaicism of the heart muscle. (Figure 2.2 B) Recombination was not detected in other tissues. Quantitative RT-PCR analysis using total RNA prepared from left ventricles of three-month old mice revealed that the expression of $Egfr$ was significantly lower in $Egfr$ CKO mice compared to their wild-type littermates. (Figure 2.2 C) Analysis of genotypes of offspring showed that $Egfr$ CKO mice were present at the expected Mendelian ratios, indicating that loss of EGFR in cardiomyocytes does not cause embryonic lethality. (Data not shown) In order to assess the

recombination efficiencies, we designed a recombination specific Taqman assay, *Egfr* KO, with

primer and the probes located Intron 2, which is deleted in *Egfr^A*. Quantitative RT-PCR using

this assay in DNA extracted from LV showed various recombination efficiencies in different age

groups with the lowest efficiency in one-year old mice, indicating that some mice with high

recombination efficiency likely died before one year of age. (Figure 2.2 D) Consistent with this

result, survival analysis showed that only 40% of *Egfr* CKO mice live to one year (n=35)

compared with 76.9% for wild-type controls (n=26), and 75% of *Egfr* CKO mice live to six

months of age (n=12) compared with 100% of controls (n=8). (Data not shown)

Egfr CKO **mice develop severe heart dysfunction**

Although *Egfr* CKO mice were born at Mendelian frequencies with normal cardiac

morphogenesis at birth, and can live to adulthood. The life-span for the majority of *Egfr* CKO

mice are less than one year because of sudden death. Physiological examination of the hearts

from adult *Egfr* CKO mice using echocardiography showed an age-related dilated

cardiomyopathy, which was most severe in one-year old *Egfr* CKO mice. (Figure 2.3 A,B) At

three months of age, *Egfr* CKO mice showed normal cardiac function, which is reflected by

fractional shortening (FS%) with normal left ventricular internal dimension, diastolic (LVID,d),

and left ventricular posterior wall, diastolic (LVPW,d). At six months of age, cardiac function

was repressed significantly in *Egfr* CKO mice. However, LV diameter and LV wall thickness

were still normal at six months of age when compared with wildtype controls. Interestingly, at

one year of age, the left ventricle diameter dilated dramatically to reach an average value of 4.5

mm in the *Egfr* CKO mice compared with 2.8 mm in the wildtype mice. (Figure 2.3 C-E)

Moreover, sudden death of one-year-old *Egfr* CKO mice was also observed during

echocardiographic examinations, which is a common symptom for dilated cardiomyopathy patients.

Histology of adult *Egfr* CKO hearts revealed several abnormal features that are common with heart from dilated cardiomyopathy patients. Ventricular chamber dilation was evident in *Egfr* CKO mice at one year of age, as manifested by the significant reduction in LV thickness and the increased LV diameter. (Figure 2.4 A-B) Moreover, heart-to-body weight ratios in mice at one year of age were higher in *Egfr* CKO than control mice despite having similar body weights (41.83±2.6 g for CKO mice vs 39.7±1.8 g for control mice), indicating a hypertrophic growth in the heart. (Figure 2.4 C) Consistent with the increased heart-to-body weight ratio, the size of cardiomyocytes from CKO was significantly enlarged at six months and one year of age but not at three months. (Figure 2.4 D-F) Additionally, extensive interstitial fibrosis and atrial thrombus were also observed in the histological section from one-year-old *Egfr* CKO mice. (Figure 2.4 G,I)

The expression of several hypertrophy-related genes, including atrial nautriuretic peptide (*Nppa)* and brain nautriuretic peptide (*Nppb*) have been used as sensitive and consistent biomarkers for cardiac hypertrophy in humans and mice.[28] The re-expression of ventricular NPPA and NPPB is known as a marker for the induction of the embryonic gene program in cardiomyocyte hypertrophy. The expression of NPPA and NPPB were not different between *Egfr* CKO and control mice at three months of age. NPPA and NPPB appeared up-regulated in the LV of *Egfr* CKO mice at six months of age compared with controls, but only NPPA reached statistical significance (p value < 0.01 for NPPA, and p value < 0.09 for NPPB). For mice at one year of age, NPPA and NPPB expression were both dramatically increased in *Egfr* CKO LVs

compared to controls. (Figure 2.5 A,B) This expression pattern across age was correlated with cardiac function and cardiomyocyte cell size.

Severity of cardiac dysfunction in *Egfr* CKO mice associates with recombination efficiency

The recombination efficiency varied among mice from 5-70%. (Figure 2.2 D) Because the heart is a mixture of different cell types including cells other than cardiomyocytes, the recombination efficiency for MHC-cre mice in total LV cannot be 100%. Since fractional shortening (FS%), a measurement of the pumping function of the heart, is the most direct and sensitive parameter for cardiac dysfunction, correlation between the recombination efficiency and cardiac dysfunction using linear regression analysis for Egfr^{wt} % (= 1- recombination efficiency) vs FS% for *Egfr* CKO mice at three months, six months and one year of age. (Figure 2.6 A-C)

Although the correlation between Egfr^{wt} % and FS% was not significant at three months and one year of age groups, Egfr^{wt}% showed a positive correlation with FS% in the six months of age group (p value < 0.0107; $R^2 = 0.4951$). (Figure 2.6 B) The onset for cardiac dysfunction in *Egfr* CKO mice occurs after three months of age, which is why no correlation was observed at young ages. Moreover, because only 40% of *Egfr* CKO mice live to one year, the correlation between recombination efficiency and FS% was likely weakened by loss of mice with high recombination levels die before one year of age.

Based on recombination efficiencies, EGFR activity is likely not completely inactivated in all cardiomyocytes. Therefore, the *Egfr* CKO model may under-represent the deleterious cardiac effects caused by chronic exposure to anti-EGFR drugs. Interestingly, even for those mice with low recombination efficiencies, cardiac function was also suppressed at one year of age due to the fact that cardiomyocytes work as a unit to maintain normal cardiac function.

Normal aortic valves in *Egfr* CKO mice

EGFR has vital roles in cardiac valve formation. Mice homozygous for *Egfr^{wa2}*, a hypormorphic mutation in *Egfr*, develop semi-lunar valve thickening and aortic stenosis (AS). In order to rule out the possibility that cardiac dysfunction observed in *Egfr* CKO mice is due to AS, the morphology and function of aortic valves was assessed. Increased peak velocity across the aortic valve is a feature of aortic stenosis. Doppler tracing taken at the level of the aortic root revealed no peak velocity differences between *Egfr* CKO mice and littermate controls indicating normal aortic valve function in *Egfr* CKO mice. (Figure 2.7 A) Aortic valve diameter was also measured from H&E stained sections. *Egfr* CKO mice had similar aortic valve morphology and thickness compared with wild-type controls. (Figure 2.7 B)

The progression of cardiac dysfunction was assessed by correlating FS% with heart-to-body weigh ratios (HW/BW ratio) in *Egfr* CKO and wildtype mice at three months, six months and one-year of age. (Figure 2.8) In the three-month-old group, the majority of *Egfr* CKO mice displayed normal FS% and HW/BW ratios except for one mouse, which had a decreased FS% and higher HW/BW ratio. (Figure 2.8 A) For six-month-old mice, most of the *Egfr* CKO mice showed impaired cardiac function with reduced FS%, but HW/BW ratios similar to wildtype controls. (Figure 2.8 B) For one-year-old mice, all *Egfr* CKO mice displayed decreased FS%, and several *Egfr* CKO mice also had an increased HW/BW ratio compared with controls. (Figure 2.8 C) Therefore, the pathological progression for *Egfr* CKO mice appears that mice have impaired cardiac function around or before six months of age, then the impaired cardiac function triggers hypertrophy in cardiacmyocytes, and increased HW/BW ratios to compensate for the damaged heart function. However, in the situation of aortic stenosis, which would induce pressure overload in the LV, the heart becomes hypertrophic first with normal cardiac function,

then progresses to a late stage dilated cardiomyopathy with reduce FS% and high HW/BW. This pathological progression of *Egfr* CKO mice suggests that AS is not the cause of cardiac dysfunction in *Egfr* CKO mice.

Apoptosis rates for cardiomyocytes is unchanged in *Egfr* CKO mice

Loss of cardiomyocytes can increase cardiac stress and can cause cardiac dysfunction and cardiomyocyte hypertrophy. Because activation of EGFR is known to confer cardio-protection by activating cell survival signaling pathways[22], Quantitative RT-PCR and TUNEL assays were performed to investigate whether apoptosis rates are increased in *Egfr* CKO mice.[29] To minimize effects on apoptosis caused by impaired cardiac function, we focus on the *Egfr* CKO mice at three months of age when they display no overt signs of heart dysfunction. Our results show there was no significant difference in TUNEL-positive cardiac cells between *Egfr* CKO and wildtype controls mice (Figure 2.9 A). Consistent with results from the TUNEL assay, expression of the pro-apoptotic gene *Bax* was also not significantly altered in *Egfr* CKO compared with control mice (Figure 2.9B).

Effect of *Egfr* deletion on gene expression in the hearts of conditional knockout mice

To identify target genes of EGFR signaling in the heart, RNAs from the LVs of *Egfr* CKO and wildtype mice were isolated and analyzed using Agilent microarrays. To avoid effects on gene expression caused by secondary changes such as cardiac hypertrophy, three-month-old mice were used (n = 6 for *Egfr* CKO, n = 6 for wildtype controls). The microarrays confirmed down-regulation of *Egfr* in the LV of *Egfr* CKO mice. No other ERBB family members showed altered expression between the *Egfr* CKO and wildtype mice. Although the expression of ACTA, a cardiac hypertrophy biomarker, was significantly up-regulated, expressions of other hypertrophy markers, such as NPPA and NPPB, were not altered. Pathway analysis did not

show enrichment for the apoptosis pathway, consistent with TUNEL results, but did show over-representation of genes associated with the adhesions junction (*p* value = 0.02), including *Ep300*, *Actb*, catenin and *Snai2*.

Egfr CKO mice are more sensitive to pressure overload

To determine the effect of cardiac-specific Egfr inactivation on the heart's response to stress, pressure overload was induced by transverse aortic constriction (TAC) in three month-old wild-type and CKO male mice. Cardiac function was assessed in TAC mice and sham controls of each genotype by echocardiography. By two weeks post-surgery, TAC control mice developed compensated hypertrophy, reflected by increased contractile function, decreased LVEDD and LVEDS, and increased wall thickness (Figure 2.10). However, hearts from *Egfr* CKO mice showed reduced FS% without compensating with increased pressure in the LV after aortic banding. Interestingly, a subset of *Egfr* CKO mice developed dilated cardiamyopathy (20%, n = 10) two weeks post aortic binding, but none of the wild-type mice showed dilated heart even at six weeks post surgery (n = 8).

II.5   Discussion

Here a mouse model is described in which cardiomyocyte-restricted deletion of *Egfr* leads to dilated cariomyopathy. Although EGFR is known to have an essential role in aortic valve development, *Egfr* CKO mice had normal valve function ruling out the possibility that observed cardiac dysfunction was secondary to valve abnormalities.[24] The data reported here shows that EGFR is also important for maintaining cardiac function in adult hearts. Most *Egfr* CKO mice show no morphological defects at three months of age, unlike mice from *Errb2* CKO (MHL2V Cre) that have severely dilated hearts at three months of age. This result may reflect a

protective role for EGFR signaling but not ERBB2 in hearts of young mice, or alternatively suggest that although important, EGFR may be a minor pathway for maintaining cardiac function as opposed to the ERBB2 pathway. Also, the expression level of ERBB2 is higher than EGFR in adult hearts.[11] Moreover, anti-ERBB2 therapies shows more prominent cardiotoxicity than anti-EGFR therapies in breast cancer, consistent with the idea that EGFR may play a minor role compared with ERBB2 in adult heart homeostasis.[30]

Recombination efficiency varies among *Egfr* CKO mice, and this recombination efficiency is significantly correlated with a deleterious outcome. Also, even in mice with very low recombination rates, cardiac function was also impaired with aging indicating that different cells work as a unit in the heart. Because most of the *Egfr* CKO mice did not completely delete the *Egfr* allele in cardiomyocytes, the *Egfr* CKO model may underestimate the negative effect in adult hearts lacking EGFR activity.

Egfr CKO mice display a complex cardiac dysfunction, including cardiomyocyte hypertrophy, left ventricular dilation and decreased pumping function. The progression of pathology in cardiac dysfunction appears to be cardiomyocyte and ventricular dilation followed by decreased pumping function. Hypertrophy is an indicator for cardiac stress, whether induced by exercise in healthy individuals or pathological alterations in patients. Hypertrophy in a healthy individual often accompanies an increased cardiac pumping function, however, this is frequently decreased in cardiomyopathy patients. The hypertrophy observed in the *Egfr* CKO mice can thus be interpreted as a secondary response to an underlying functional deficit in the heart.

Loss of cardiomyocytes can also induce cardiac stress and lead to impaired cardiac function and hypertrophy.[31,32] EGFR signaling is known to confer cardioprotection by activating

cell survival pathways in heart by chronic stimulation of beta-adrenergic receptors.[29] However, no increased apoptosis was observed in hearts of adult *Egfr* CKO mice. Because recombination induced by Cre was not complete, the hearts of *Egfr* CKO mice consisted of a mosaic of *Egfr^{wt/wt}*, *Egfr^{-/wt}* and *Egfr^{-/-}* cardiomyocytes. Using quantitative RT-PCR with LV RNA from hearts of six-month-old *Egfr* CKO mice, which have impaired cardiac function, have a similar distribution of *Egfr^{wt}* percentage as from the three-month old *Egfr* CKO mice. (Figure 2.2 D) This data indicated that there was no preferential loss of *Egfr^{-/-}* cardiomyocytes. We did detect an up-shift of the percentage of *Egfr^{wt}* in the hearts of one-year-old *Egfr* CKO, but this was most likely a loss of mice with low a percentage of remaining *Egfr^{wt}* alleles with high numbers of *Egfr^{-/-}* cardiomyocytes because survival rate for one-year-old *Egfr* CKO was only 40%. Thus, mechanisms other than apoptosis appear to cause cardiac dysfunction in *Egfr* CKO mice, such as impaired contractility.

The expression of ACTA increased in hearts of *Egfr* CKO mice at three months of age. Up-regulation in the expression of ACTA has been previously noted in various models of cardiac dysfunction indicating existence of some sort of stress in the heart. Also, pathway analysis showed that genes associated with adhesive junctions are significant enriched in the microarray data. Others have shown that dysregulation of cell adhesion causes cardiac arrhythmogenesis and dysfunction. It is possible that abnormal adhesive junctions in the hearts of *Egfr* CKO mice might cause the severe cardiac dysfunction in adult heart.

The essential role of EGFR in cardiomyocytes for maintaining normal cardiac homeostasis suggests that chronic exposure to anti-EGFR drugs may induce cardiomyopathy. To date, most anti-EGFR drugs are only used for late stage cancer patients with short life expectancy, so cardiotoxicity is not prominent. This is also consistent with the late onset of

cardiac dysfunction in the *Egfr* CKO model. Also, *Egfr* CKO mice showed a poor response to pressure overload, which may suggest that anti-EGFR therapy combined with chemotherapy, may induce more potent cardiotoxicity.

Figure 2.1: Cre expression in *MHC$^{cre/+}$* mice. Whole heart X-gal-stained for *R26R* mice (A) and *MHC$^{cre/+}$/R26R* mice (B), X-gal-stained for *R26R* heart section (C) and *MHC$^{cre/+}$/R26R* heart section (D).
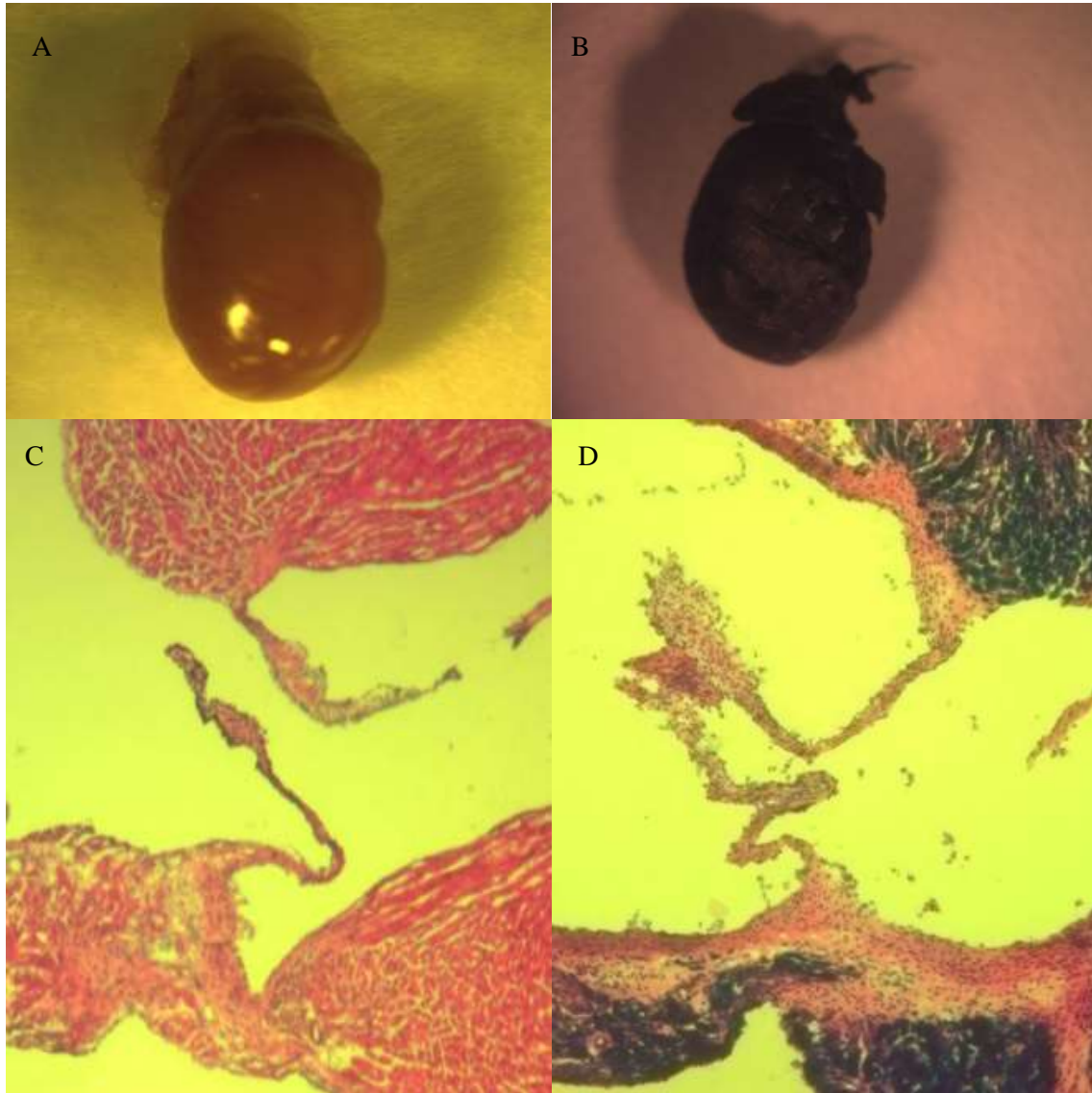
Figure 2.2: Cre-mediated mutation of *Egfr* in cardiomyocyte. (A) Schematic representation of the *Egfr* locus with *loxp* sequence (black arrowheads) and the position of primer used for PCR in (B). (B) PCR using primers indicated in (A) in heart and spleen DNA of $Egfr^{f/f}: MHC^{-/-}$ and $Egfr^{f/f}: MHC^{-/+}$ mice. Positions of $Egfr^{flox}$ and $Egfr^{\Delta}$ allele fragments are indicated, and PCR for β-casein-1 were used as an internal control. (C) Relative fold changes in *Egfr* in the LV of *Egfr* CKO mice compared to wildtype. (D) Recombination efficiencies in different age group of *Egfr* CKO mice. Subset of CKO mice (20%, n=10) would develop dilated heart after two weeks of aortic banding, however, none of wild-type mice developed dilated cardiomyopathy even at 6 weeks after aortic binding.
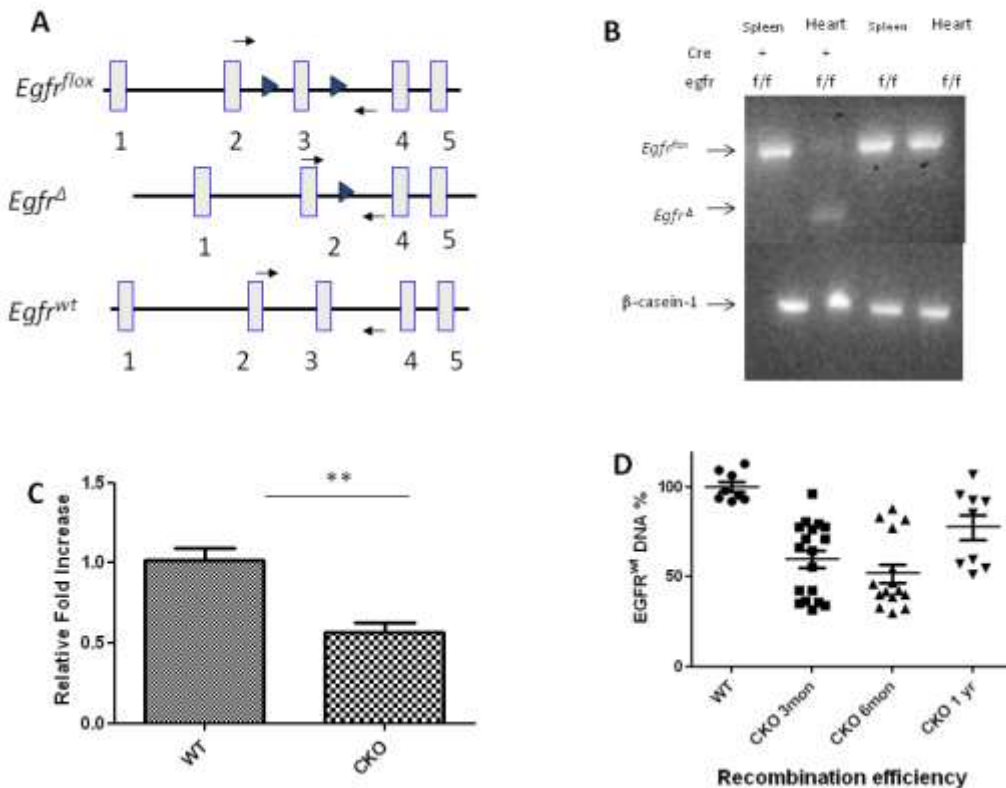
Figure 2.3: *Egfr* CKO mice develop marked deficits in heart function. Representative examples of echocardiography image of left ventricle from one year old wildtype control (A) and age matching *Egfr* CKO mice (B). Fractional shortening (C), left ventricular internal dimension, diastolic (LVID,d) (D) and left ventricular posterior wall, diastolic (LVPW,d) of wildtype and *Egfr* CKO mice with the indicated ages. *Egfr* CKO mice develop dilated cardiomyopathy at the age of one year old, but impaired cardiac function, which is reflected in reduced FS, from age of six months. FS%, percent fractional shortening; LVID,d, left ventricular internal dimension, diastole; LVPW,d, left ventricular posterior wall, diastole.
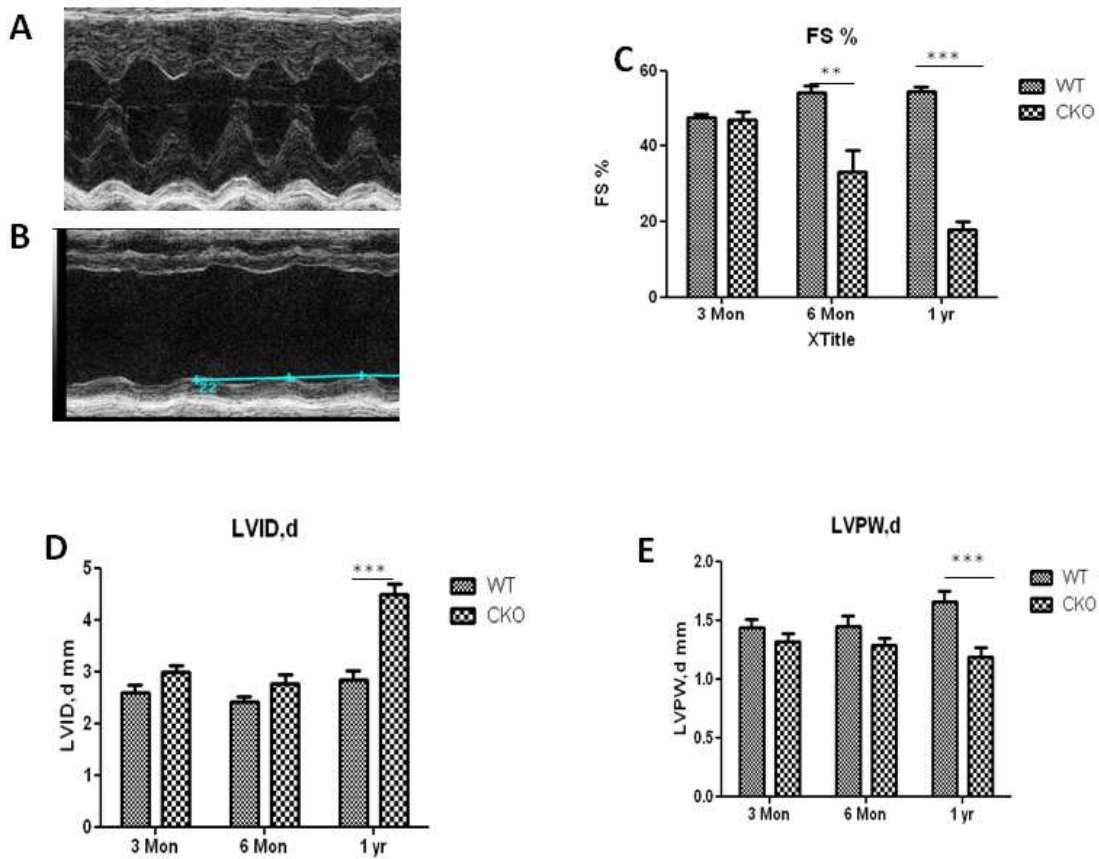
Figure 2.4: Ventricular dilation and myofiber hypertrophy in *Egfr* CKO mice.

Hematoxylin/eosin-stained (H&E) sections of the entire heart of one- year-old *Egfr* CKO (A) and wildtype control mice (B). Note the dilated ventricle chamber in CKO mice. Heart-to-body weight ratios (C) and cardiomyocyte size (D) increased with aging in CKO mice. High magnifications of H&E stained sections with hypertrophy apparent in CKO mice (E) but not controls (F). Masson's trichrome stained sections from LV free wall with extensive interstitial fibrosis in CKO mice (G) but not controls (H). Representative H&E stained section showing Atrial thrombus in CKO mice (I).
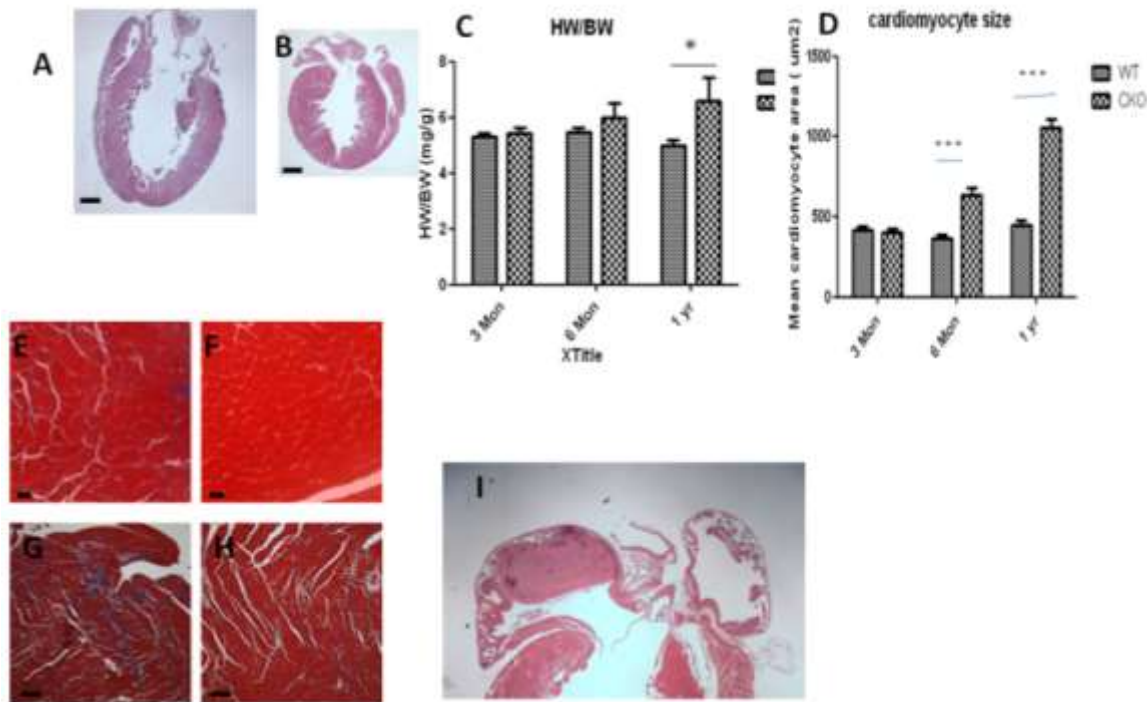
Figure 2.5: Comparison of relative expression of cardiac hypertrophy markers in LV. (A) Expression of NPPA was significantly increased in *Egfr* CKO mice at the age of six months and one year compared with age-matching wildtype littermates. (B) NPPB was significantly up-regulated in CKO mice at the age of one year compared with controls.
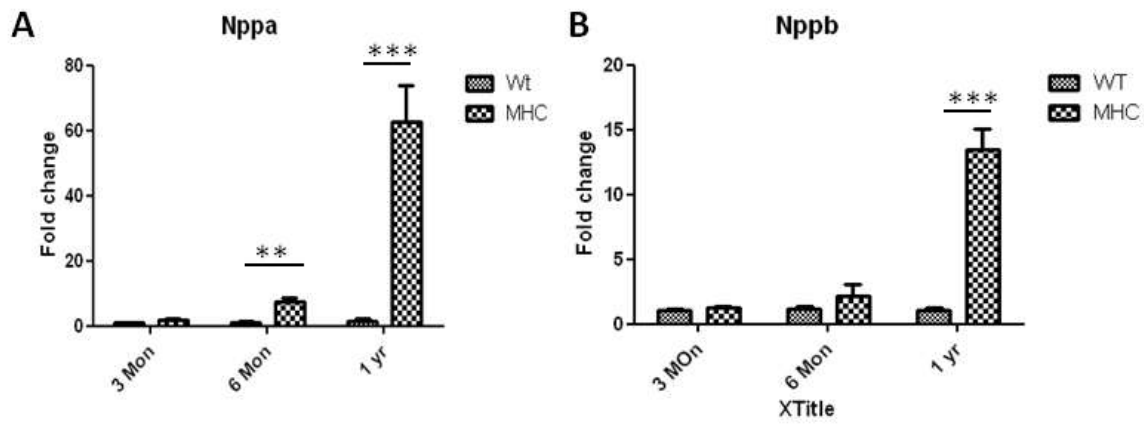
Figure 2.6: Correlation between FS% and Egfr^{wt}%. (A) Linear regression analysis showed that the correlation between FS% and Egfr^{wt}% was not significant (p value = 0.288, r^2 = 0.0712). (B) The correlation was significant (p value = 0.0107, r^2 = 0.4951), (C) The correlation was not significant (p value = 0.6937, r^2 = 0.02351). FS%, percent fractional shortening; EGFR^{wt}%, percentage of *Egfr* wildtype allele.
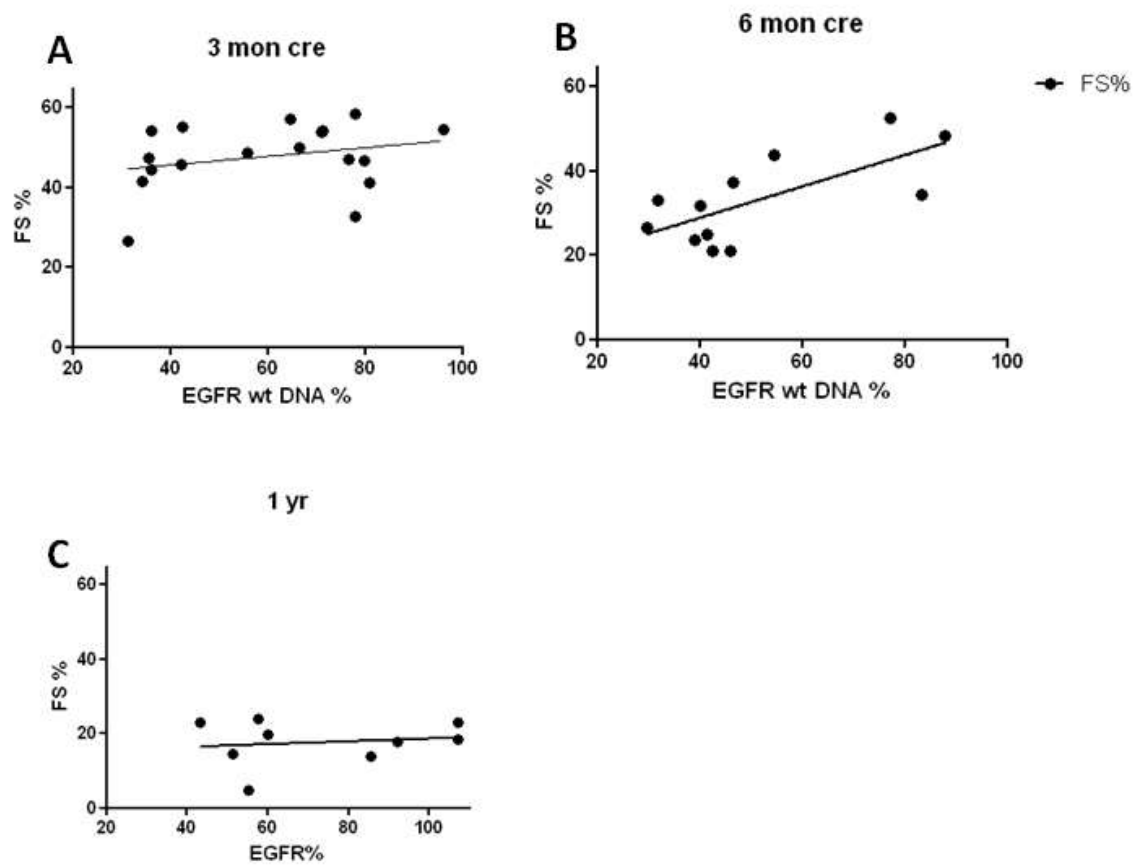
Figure 2.7: Comparison of aortic valve function and morphology between *Egfr* CKO and wildtype mice. (A) Representative Doppler tracing from *Egfr* CKO and wildtype mice at the level of the aortic root. (B) Representative H&E stained sections of the thickest region of aortic valves from *Egfr* CKO and wildtype mice.
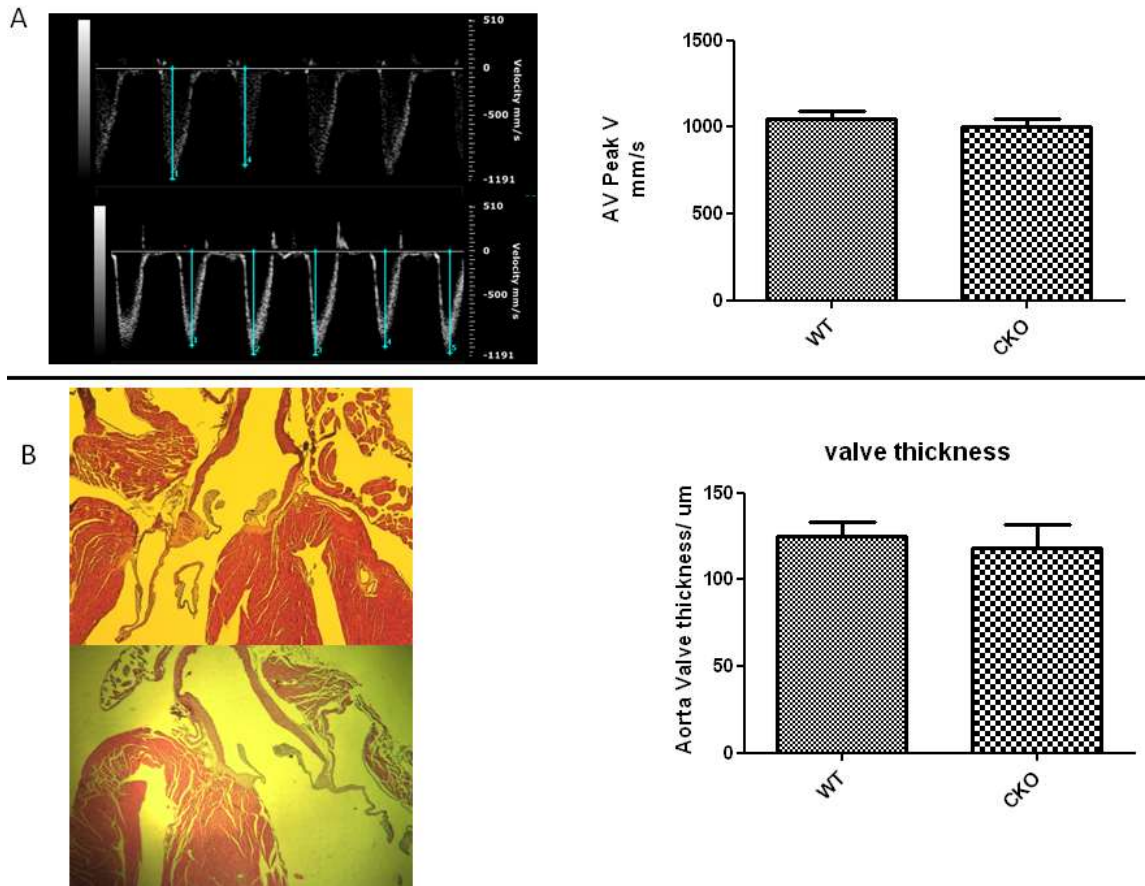
Figure 2.8: Cardiac pathology progression in *Egfr* CKO mice. FS% was plotted with HW/BW at the age of three months (A), six months, (B) and one year (C). FS%, percent fractional shortening; HW/BW, heart-to-body weight ratio.
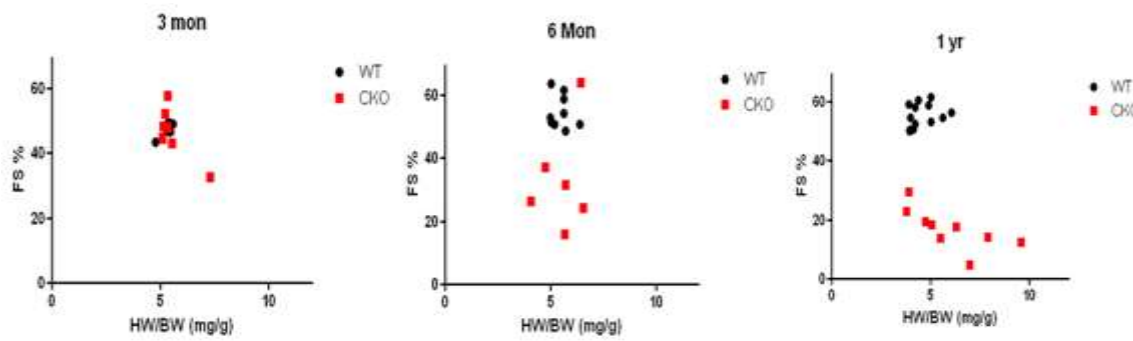
Figure 2.9: Apoptosis in the hearts of *Egfr* CKO and wildtype mice. (A) TUNEL assays. (B) Expression of pro-apoptotic gene *Bax*.
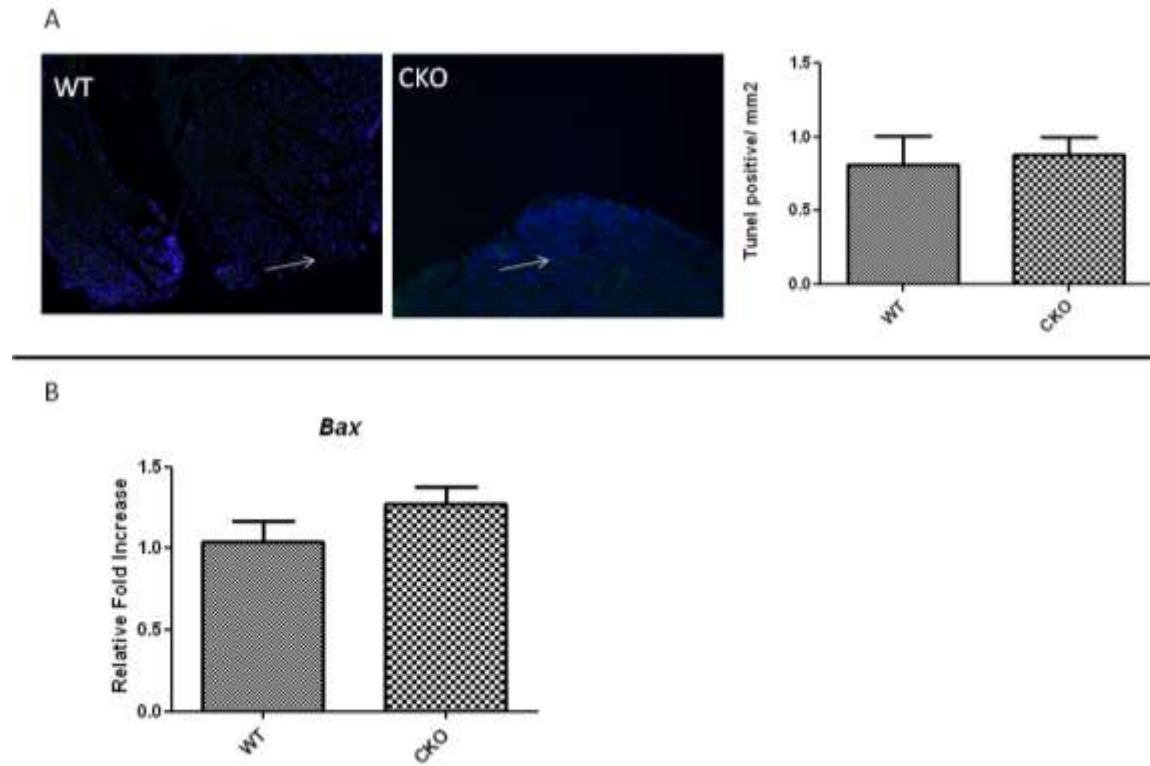
Figure 2.10: Deterioration of cardiac function in *Egfr* CKO mice following TAC treatment. Representative M-mode tracing taken from long-axis before and two weeks post surgery from *Egfr* CKO and wildtype mice. TAC, transverse aortic constriction; FS%, percent fractional shortening.
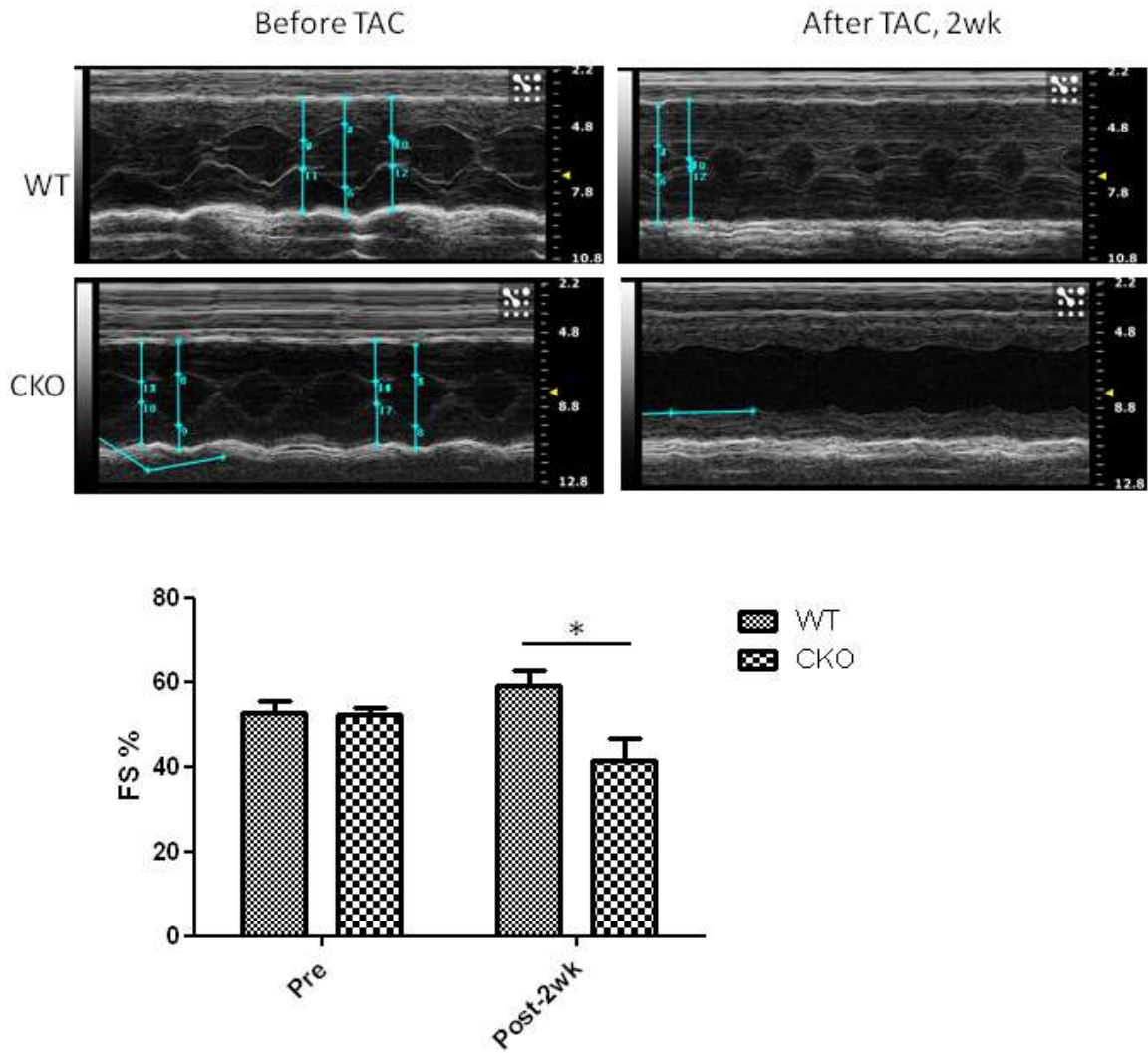
REFERENCES

1.   Gullick, W.J. Type I growth factor receptors: current status and future work. *Biochem Soc Symp* **63**, 193-8 (1998).

2.   Wells, A. EGF receptor. *Int J Biochem Cell Biol* **31**, 637-43 (1999).

3.   Weiss, F.U., Daub, H. & Ullrich, A. Novel mechanisms of RTK signal generation. *Curr Opin Genet Dev* **7**, 80-6 (1997).

4.   Schlessinger, J. Cell signaling by receptor tyrosine kinases. *Cell* **103**, 211-25 (2000).

5.   Sharma, S.V., Bell, D.W., Settleman, J. & Haber, D.A. Epidermal growth factor receptor mutations in lung cancer. *Nat Rev Cancer* **7**, 169-81 (2007).

6.   Levy, D., Salomon, M., D'Agostino, R.B., Belanger, A.J. & Kannel, W.B. Prognostic implications of baseline electrocardiographic features and their serial changes in subjects with left ventricular hypertrophy. *Circulation* **90**, 1786-93 (1994).

7.   Woodburn, J.R. The epidermal growth factor receptor and its inhibition in cancer therapy. *Pharmacol Ther* **82**, 241-50 (1999).

8.   Nicholson, R.I., Gee, J.M. & Harper, M.E. EGFR and cancer prognosis. *Eur J Cancer* **37 Suppl 4**, S9-15 (2001).

9.   Weinstein, I.B. & Joe, A.K. Mechanisms of disease: Oncogene addiction--a rationale for molecular targeting in cancer therapy. *Nat Clin Pract Oncol* **3**, 448-57 (2006).

10.   Chen, M.H., Kerkela, R. & Force, T. Mechanisms of cardiac dysfunction associated with tyrosine kinase inhibitor cancer therapeutics. *Circulation* **118**, 84-95 (2008).

11.   Crone, S.A. et al. ErbB2 is essential in the prevention of dilated cardiomyopathy. *Nat Med* **8**, 459-65 (2002).

12. Uray, I.P. et al. Left ventricular unloading alters receptor tyrosine kinase expression in the failing human heart. *J Heart Lung Transplant* **21**, 771-82 (2002).

13. Rohrbach, S., Niemann, B., Silber, R.E. & Holtz, J. Neuregulin receptors erbB2 and erbB4 in failing human myocardium -- depressed expression and attenuated activation. *Basic Res Cardiol* **100**, 240-9 (2005).

14. Rohrbach, S. et al. Neuregulin in cardiac hypertrophy in rats with aortic stenosis. Differential expression of erbB2 and erbB4 receptors. *Circulation* **100**, 407-12 (1999).

15. Schneider, J.W., Chang, A.Y. & Rocco, T.P. Cardiotoxicity in signal transduction therapeutics: erbB2 antibodies and the heart. *Semin Oncol* **28**, 18-26 (2001).

16. Schneider, J.W., Chang, A.Y. & Garratt, A. Trastuzumab cardiotoxicity: Speculations regarding pathophysiology and targets for further study. *Semin Oncol* **29**, 22-8 (2002).

17. Ewer, M.S., Gibbs, H.R., Swafford, J. & Benjamin, R.S. Cardiotoxicity in patients receiving transtuzumab (Herceptin): primary toxicity, synergistic or sequential stress, or surveillance artifact? *Semin Oncol* **26**, 96-101 (1999).

18. Ozcelik, C. et al. Conditional mutation of the ErbB2 (HER2) receptor in cardiomyocytes leads to dilated cardiomyopathy. *Proc Natl Acad Sci U S A* **99**, 8880-5 (2002).

19. Garcia-Rivello, H. et al. Dilated cardiomyopathy in Erb-b4-deficient ventricular muscle. *Am J Physiol Heart Circ Physiol* **289**, H1153-60 (2005).

20. Daub, H., Weiss, F.U., Wallasch, C. & Ullrich, A. Role of transactivation of the EGF receptor in signalling by G-protein-coupled receptors. *Nature* **379**, 557-60 (1996).

21. Shah, B.H. & Catt, K.J. Matrix metalloproteinase-dependent EGF receptor activation in hypertension and left ventricular hypertrophy. *Trends Endocrinol Metab* **15**, 241-3 (2004).

22. Pareja, M., Sanchez, O., Lorita, J., Soley, M. & Ramirez, I. Activated epidermal growth factor receptor (ErbB1) protects the heart against stress-induced injury in mice. *Am J Physiol Regul Integr Comp Physiol* **285**, R455-62 (2003).

23.   Barrick, C.J. et al. Reduced EGFR causes abnormal valvular differentiation leading to calcific aortic stenosis and left ventricular hypertrophy in C57BL/6J but not 129S1/SvImJ mice. *Am J Physiol Heart Circ Physiol* **297**, H65-75 (2009).

24.   Chen, B. et al. Mice mutant for Egfr and Shp2 have defective cardiac semilunar valvulogenesis. *Nat Genet* **24**, 296-9 (2000).

25.   Agah, R. et al. Gene recombination in postmitotic cells. Targeted expression of Cre recombinase provokes cardiac-restricted, site-specific rearrangement in adult ventricular muscle in vivo. *J Clin Invest* **100**, 169-79 (1997).

26.   Hu, P. et al. Minimally invasive aortic banding in mice: effects of altered cardiomyocyte insulin signaling during pressure overload. *Am J Physiol Heart Circ Physiol* **285**, H1261-9 (2003).

27.   Liu, F.F. et al. Heterozygous knockout of neuregulin-1 gene in mice exacerbates doxorubicin-induced heart failure. *Am J Physiol Heart Circ Physiol* **289**, H660-6 (2005).

28.   Simpson, P.C., Long, C.S., Waspe, L.E., Henrich, C.J. & Ordahl, C.P. Transcription of early developmental isogenes in cardiac myocyte hypertrophy. *J Mol Cell Cardiol* **21 Suppl 5**, 79-89 (1989).

29.   Noma, T. et al. Beta-arrestin-mediated beta1-adrenergic receptor transactivation of the EGFR confers cardioprotection. *J Clin Invest* **117**, 2445-58 (2007).

30.   Fuchs, I.B. et al. Analysis of HER2 and HER4 in human myocardium to clarify the cardiotoxicity of trastuzumab (Herceptin). *Breast Cancer Res Treat* **82**, 23-8 (2003).

31.   Hirota, H. et al. Loss of a gp130 cardiac muscle cell survival pathway is a critical event in the onset of heart failure during biomechanical stress. *Cell* **97**, 189-98 (1999).

32.   Chien, K.R. Stress pathways and heart failure. *Cell* **98**, 555-8 (1999).

Chapter III: GENETIC MODIFIER LOCUS AFFECTING LEFT VENTRICULAR HYPERTROPHY IN THE *EGFR^WA2* MOUSE MODEL OF AORTIC STENOSIS[1]

III.1 Overview

Left ventricular hypertrophy (LVH), or thickening of the myocardium of the left ventricle, is known as an independent risk factor for cardiac-related morbidity and mortality. Cardiovascular disease, such as aortic stenosis (AS) which chronically elevates afterload, is the main cause of LVH. A large body of evidence suggests genetic components significantly modulate the development and severity of AS-related left ventricular hypertrophy. Mice homozygous for a hypomorphic mutation in the epidermal growth factor receptor gene (*Egfr^wa2*) on a mixed genetic background were discovered to have congenitally enlarged aortic valves with mild AS. Interestingly, mice homozygous for *Egfr^wa2* on C57BL/6J (B6) and 129S1/SvImJ (129S1) inbred backgrounds showed significant strain and sex-dependent variation in LVH and progression to heart failure, with male B6-*Egfr^wa2/wa2* mice having the most severe cardiac phenotype. Using the B6 and 129S1 inbred strains, a B6129S1 F2-*Egfr^wa2/wa2* (F2-*Egfr^wa2/wa2*) population was created to genetically map *Egfr*-dependent modifiers of LVH. Linkage analysis identified one significant locus, *Edlvhq1 (Egfr-dependent left ventricular hypertrophy qtl 1)*, on Chromosome (Chr) 9 in males (LOD score ~ 4.5, p < 0.05) and one suggestive locus, *Edlvhq2,* on Chr 16 in females (LOD score ~5.1, p < 0.37) that were linked to heart weight. After

---

[1] Mice breeding and phenotyping were done by Codelia Barrick

increasing sample size, *Edlvh1* was confirmed; however, signal on Chr 16 was not replicated. By applying haplotype analysis of the candidate regions, the critical interval on Chr 9 was narrowed and candidate genes identified that may be responsible for the modifier effect on LVH. Identification of genetic modifiers using the *Egfr^wa2* disease model may provide novel mechanistic insight into the pathogenesis and progression of AS and LVH.

III.2 Introduction

Left ventricular hypertrophy (LVH), or thickening of the myocardium of the left ventricle (LV), is an independent risk factor for cardiac-related morbidity and mortality.[1-3] Although mechanical stress, growth factors, catecholamines, cytokines and primary genetic abnormalities all can induce LVH, chronically elevated after-load, which increases LV stroke work, is the most common cause. Two prevalent cardiovascular diseases that induce LVH secondary to increased after-load are Aortic stenosis (AS) and essential hypertension (EH). Clinical presentation for LVH is highly variable among different patients.[4,5,6] Although several risk factors have been proposed, increasing evidence suggests genetic components significantly modulate the development and severity of AS and EH-related LVH, as well as LVH regression with therapy.[7-14] Thus, identifying genetic factors accounting for the pathogenesis of LVH is pivotal to the successful clinical management of these common cardiovascular diseases.

Transverse aortic constriction (TAC), which leads to aortic narrowing and increased LV pressure overload, is an accepted experimental model for human cardiac response to chronic pressure overload.[15-20] C57BL/6J (B6) TAC mice have a more severe pathological outcome, including decreased survival, LVH, and earlier progression to heart failure than 129S1/SvImJ (129S1) or F1 (B6x129S1) TAC mice.[21] Since all mice shared similar environmental conditions,

this strongly suggested that genetic factors significantly modify cardiac response to increased pressure overload. However this model is not ideal for genetic analysis, since the degree of constriction, and thus induced load, can fluctuate resulting in high technical variation, which reduced consistency of results.[22,23] Therefore, to identify quantitative trait locus (QTL) that modify the hypertrophic response, a genetic model of pressure-overload induced LVH was used.

The *waved-2* allele (*Egfr^wa2*), a hypomorphic allele, encodes a single base mutation in the epidermal growth factor receptor (*Egfr/Erbb1*) gene, resulting in up to 90% reduction in receptor activity.[24] On a mixed genetic background, *Egfr^wa2/wa2* mice develop enlarged aortic valves and mild to moderate AS, but otherwise are viable and fertile, with minor coat and eye phenotypes.[25] However, this mutation shows a significant strain-dependent variability in cardiac phenotypes on the B6 and 129S1 genetic backgrounds. With similar congenital valve defects, B6-*Egfr^wa2/wa2* develop more severe cardiac hypertrophy, congestive heart failure and AS than 129-*Egfr^wa2/wa2*.[21] Since F1-*Egfr^wa2/wa2* (B6-*Egfr^wa2/+* X 129S1-*Egfr^wa2/wa2*) offspring show similar phenotype as 129-*Egfr^wa2/wa2* mice, 129S1 genetic modifiers are protective and dominant to B6 in the cardiac response to chronic pressure overload. Therefore, an F2-*Egfr^wa2/wa2* (F2 generated from crosses between B6- and 129-*Egfr^wa2/wa2*) population was created in order to map genes modifying the development of LVH.

III.3 Materials and Methods

Animals

The generation and genotyping of B6-*Egfr^wa2/wa2* and 129-*Egfr^wa2/wa2* mice have been previously described.[21] The B6-*Egfr^wa2/+* females were crossed with 129S1-*Egfr^wa2/wa2* males to generate F1-*Egfr^wa2/wa2* population. Four male and four female F1-*Egfr^wa2/wa2* mice randomly

intercrossed and generated one hundred and ninety F2 offspring. Additionally, thirty two

backcross N2 mice were generated by crossing F1-*Egfr*^{*wa2/wa2*} females and B6-*Egfr*^{*wa2/wa2*} males.

All mice experiments followed National Institutes of Health guidelines and were approved by the

University of North Carolina Institutional Animal Care and Use Committee.

Genotyping

Fifty five F2 progeny were used for analysis because their phenotypic values were greater

than 0.5 standard deviations from the mean. Since heart weight was not normally distributed, log

transformed heart weight (logHW) was used for analysis. One-way interval mapping were

performed using R/qtl package.[26] Because the mice were selected with extreme phenotypes,

significant thresholds were calculated by performing 1000 stratified permutations.[26,27]

Genome-wide Scan

Fifty five F2 progeny were used for analysis because their phenotypic values were greater

than 0.5 standard deviations from the mean. Since heart weight was not normally distributed, log

transformed heart weight (logHW) was used for analysis. One-way interval mapping were

performed using R/qtl package.[26] Because the mice were selected with extreme phenotypes,

significant thresholds were calculated by performing 1000 stratified permutations.[26,27]

Haplotype analysis

The haplotypes of regions within a 1.5 LOD interval surrounding each QTL were

compared between B6 and 129S1 using the Jackson Laboratory's Mouse Phenome Database

SNP collection (http://www.jax.org/phenome/snp.html). All SNPs are mapped to NCBI mouse

genome build 36.1 reference assembly (C57BL/6J). The C57BL/6J strain was used as the

reference strain compared to 129S1/SvImJ strain.

III.4   Results

Cardiac hypertrophy in *Egfr^{wa2/wa2}* mice is modified by genetic background

For heart and body weights showed strain-dependent differences weights in three months of age in *Egfr*^{wa2/wa2} mice. Heart weight (HW) in B6 was significantly increased compared to F1 and 129S1-*Egfr*^{wa2/wa2} mice (284.50 ±22.63 mg B6, 138.00 ±4.71 mg F1, 130.27 ±5.62 mg 129S1; *p* value < 0.0001) (Figure 3.1 A). Also body weight (BW) in adult homozygous mice was significantly increased compared to heterozygous littermates.[21] For example, three-month-old B6-*Egfr*^{wa2/wa2} mice weighed approximately 4.6% less than heterozygous littermates.

Moreover, normalized HW was significantly higher in B6-*Egfr*^{wa2/wa2} mice than F1 and 129S1-*Egfr*^{wa2/wa2} mice. (11.28 ±0.75 mg:g B6, 5.38 ±0.15 mg:g F1, 6.52±0.49 mg:g 129S1; *p* value < 0.0001) (Figure 3.1 C)

Sexual dimorphism exists in the temporal development of cardiac hypertrophy and heart failure in B6-*Egfr^{wa2/wa2}* mice

Although the hearts of B6-*Egfr*^{wa2/wa2} mice were consistently heavier than those of control littermates at all time points analyzed in both genders, stratifying B6-*Egfr*^{wa2/wa2} heart weight by gender and age revealed sexual dimorphism in survival and temporal development of severe cardiac hypertrophy. Approximately 40% of male B6-*Egfr*^{wa2/wa2} mice but only one female B6-*Egfr*^{wa2/wa2} mouse (10%) (n = 43, *Egfr*^{wa2/wa2} littermates) died at three months of age, most likely from heart failure. Although there were no significant differences between male and female mice in heart or lung weights in surviving three-month-old B6-*Egfr*^{wa2/wa2} mice, by 4-5 months male B6-*Egfr*^{wa2/wa2} mice had significantly heavier heart than female B6-*Egfr*^{wa2/wa2} mice. (Figure 3.1 D)

By nine months of age, B6-$Egfr^{wa2/wa2}$ female mice had significantly heavier heart than B6-$Egfr^{wa2/wa2}$ male mice (Figure 3.1 D), suggesting either females survived longer with hypertrophy or there was a temporal delay in the development of hypertrophy. Consistent with previous findings in TAC in B6 mice, these data suggested that female sex conferred a cardiac protective effect for hypertrophy and heart failure secondary to pressure overload.[28]

Cardiac phenotype of F2 $Egfr^{wa2/wa2}$ progeny

To further identify the effects of genetic factors on cardiac hypertrophy, F2-$Egfr^{wa2/wa2}$ progenies were generated by intercrossing F1-$Egfr^{wa2/wa2}$ mice. Because B6-$Egfr^{wa2/wa2}$ females had lactation defects, and B6-$Egfr^{wa2/wa2}$ male mice have short life span, B6-$Egfr^{wa/+2}$ dams crossed to 129S1-$Egfr^{wa2/wa2}$ sires to generate F1 progeny. With ability to support large litters, F1-$Egfr^{wa2/wa2}$ mice were subsequently intercrossed to produce 190 F2 offspring. At three months of age, both genders were equally represented in F2 panel (48.5% female, 51.5% male), indicating no obvious gender bias in survival within the F2 population. However, histogram of total distribution of gross HW (Figure 3.2 A), and scatter-plots comparing HW (Figure 3.2 B) by gender revealed a sexual dimorphism in the cardiac phenotypes among F2 mice. Consistent with the hypothesis of dominant 129S1 protective modifiers of cardiac hypertrophy, mean HW of B6 parental mice was significantly higher than all other groups. (Figure 3.2 B; ANOVA p value< 0.0001) Approximately 18% of the F2 panel had a HW > 220 mg, yet within this subset of severely affected mice, only 25% were female mice. The same trend was observed using HW:BW as the phenotypic endpoint (data not shown). Since by three months of age, the hearts of both male and female B6-$Egfr^{wa2/wa2}$ mice are enlarged, the protective 129S1 genetic modifiers must interact strongly with female gender in the F2 population.

Body weight in F2-*Egfr*$^{wa2/wa2}$ mice was normally distributed with greater variability than in parental *Egfr*$^{wa2/wa2}$ lines or F1 progeny. (Figure 3.2 C and D) In male mice, BW differed significantly among different genetic backgrounds, with the highest mean BW in F2 mice (29 ± 4g F2 *Egfr*$^{wa2/wa2}$, 27 ± 0.25g B6-*Egfr*$^{wa2/wa2}$, 28 ± 3g F1-*Egfr*$^{wa2/wa2}$, 24 ± 4g 129S1 *Egfr*$^{wa2/wa2}$; *p* value < 0.005). The mean BW of F2 female mice was within the BW range of parental and F1 female mice. Moreover, there was little correlation between HW and BW in F2 mice(Figure 3.2 E; $R^2 = 0.10$).

At three-months of age, F2-*Egfr*$^{wa2/wa2}$ mice revealed remarkable variation in cardiac hypertrophy, aortic valve size, fibrosis, and cardiac function (Table 3.1 and Figure 3.3). Since these mice were age and sex-matched littermates with same environment, this data highlights the significant contribution of genetic modifiers to cardiac phenotypes. Among these F2 mice, the most severely affected mouse (#62) showed the heaviest heart weight, depressed systolic function, enlarged LV chamber, enlarged valves, and cardiac fibrosis, replicating the phenotype of the B6-*Egfr*$^{wa2/wa2}$ parental line. In contrast, mouse #60 had normal aortic valves and cardiac function. For enlarged aortic valves in B6- and 129S1-*Egfr*$^{wa2/wa2}$ congenic lines and F1-*Egfr*$^{wa2/wa2}$ offspring, this suggests that some combination of B6 and 129S1 genetic modifiers was able to compensate for reduced EGFR activity during valvular development.

Mapping modifiers of cardiac hypertrophy

To map the genes that modify cardiac hypertrophy, progeny from the F2 intercross were used for linkage analysis. An initial genome screen included 56 progeny with extreme high and low ends of the heart weight distribution curve (> 0.5 STD). No markers reached suggestive or significant thresholds when the entire cohort was analyzed using HW as the phenotypic endpoint. However, when gender was used as a covariate, two suggestive QTLs for HW were identified on

Chromosome (Chr) 9 with a peak LOD score of 4.5 at rs13480120, named *Edlvhq1* (*Egfr-dependent left ventricular hypertrophy qtl 1*), and a second QTL, named *Edlvhq2,* with a peak LOD score of 4.47 at rs3696981. (Figure 3.4)

By partitioning the panel by sex, *Edlvhq1* was found to be significantly associated with heart weight only in male mice. An effect plot reveals that mice homozygous for the B6 allele of *Edlvhq1* has a heavier heart than mice heterozygous or homozygous for the 129S1 allele, which is consistent with previous observations that the 129S1 allele is dominant to the B6 allele. (Figure 3.5C) Also, whole-genome scans on the female population showed the suggestive QTL on Chr 16 to be female specific, and identified two additional female-specific putative modifiers on Chr 2 ($p < 0.37$) and Chr 11 ($p < 0.37$). (Figure 3.6 A) The modifier associated with the Chr 11 marker (rs13480881) is located closely to the *Egfr* gene. Therefore the signal for this modifier was likely an effect of selection for *Egfr^{wa2}* during generation of the congenic lines. The suggestive modifier on Chr 2 had its highest LOD score calculated from an imputed marker located in a 10 cM interval between rs13476535 and rs6367022 indicating this maybe a false positive. (Figure 3.6 B) For the QTL on Chr 16 in females, the effect plot at marker rs3696981 showed an additive effect, with B6 alleles being associated with heavier heart weights.

To confirm these results, an additional 89 mice were genotyped that also had an extreme phenotype for *Edlvhq1* at marker rs3696981 on Chr 9 and for *Edlvhq2* at marker rs3696981 on Chr 16. For *Edlvhq1*, an ANOVA test showed significant differences in heart weight ($p = 0.014$) among genotypes of male mice. (Figure 3.7 A) However, there was no significant association between the *Edlvhq2* on Chr 16 and heart weigh ($p = 0.094$), indicating that this association was not replicated. (Figure 3.7 B)

Haplotype analysis for C57BL/6J versus 129S1/SvImJ strains within candidate QTL regions

Haplotype analysis comparing B6 and 129S1 genomes was performed to narrow the candidates for *Edlvhq1* on Chr 9. Regions spanning a 1.5 LOD confidence interval around *Edlvhq1* was identified (Figure 3.8), and the underlying haplotypes revealed one major region spanning approximately 4Mb with high SNP diversity between B6 and 129S1. The marker with the highest LOD score (rs13480120, LOD 4.5) is located at 30.3 Mb, approximately 2Mb away from the candidate regions. There are approximately thirteen genes located in this region, all of which have SNPs that differ between B6 and 129S1 strains within non-coding regions. Two of these genes have known SNP variants within the coding regions of the gene: kin of IRRE like 3 (*Kirrel3*) and ST3 beta-galactoside alpha-2,3-sialyltransferase 4 (*St3gal4*).

III.5   Discussion

Using a genetically sensitized disease model, a major modifier locus on Chr 9 was localized that is associated with cardiac hypertrophy arising from chronic pressure overload. This locus, denoted *Edlvhq1*, only modulates hypertrophic response in male F_2-*Egfr*$^{wa2/wa2}$ mice, consistent with the sexual dimorphism of the cardiac phenotypes in the F_2 progeny and B6 parental congenic line. The effect plots for *Edlvh1* supported the dominant effect of the 129S1 resistance allele to the cardiac hypertrophy phenotype in the *Egfr*^{wa2} mutant model. (Figure 3.5 C)

Comparison of the B6 and 129S1 haplotypes revealed one regions of high SNP variability within the 1.5 LOD CI for *Edlvh1* on Chr 9. Within this highly variable region reside several genes that are reported to influence EGFR activity, inflammation, or cardiac development.

To assess the candidate genes for the *Edlvhq1* locus, allele specific PCR can be performed to identify possible differential expression from B6 allele and 129S1 allele in F1 *Egfr^{wa2/wa2}* mice.

Based on phenotypes from parental strains, LVH modifiers can function through either anti-arotic stenosis or anti-hypertrophy induced by pressure overload, or both. The 129-*Egfr^{wa2/wa2}* mice displayed a thinner aortic valve cusp than B6-*Egfr^{wa2/wa2}* mice. Moreover, 129 mice with TAC surgery have a better pathological outcome than B6 TAC mice, indicating that 129 modifiers may protect the heart from pressure overload with normal EGFR function.

With the increases in life expectancy of patients, some types of cancers tend to be treated as a chronic disease. However as shown in Chapter 2, EGFR is required to maintain normal cardiac function. Therefore, identification of genetic modifiers using the *Egfr^{wa2}* model may help to screen patients with high risk for anti-EGFR treatment, and help to define the role of EGFR in the pathogenesis of common cardiac diseases.

Figure 3.1: Comparison of heart weight (HW), body weight (BW), and normalized heart weight (HW:BW) by different genetic background in three-month-old $Egfr^{wa2/wa2}$ mice. A) HW, B) BW, C) HW:B. D) Distribution of heart weight by age (in months) in B6-$Egfr^{wa2/wa2}$ male (solid circle) and female (open circle) mice. *$p < 0.05$, **$p < 0.01$, ****$p < 0.0001$.
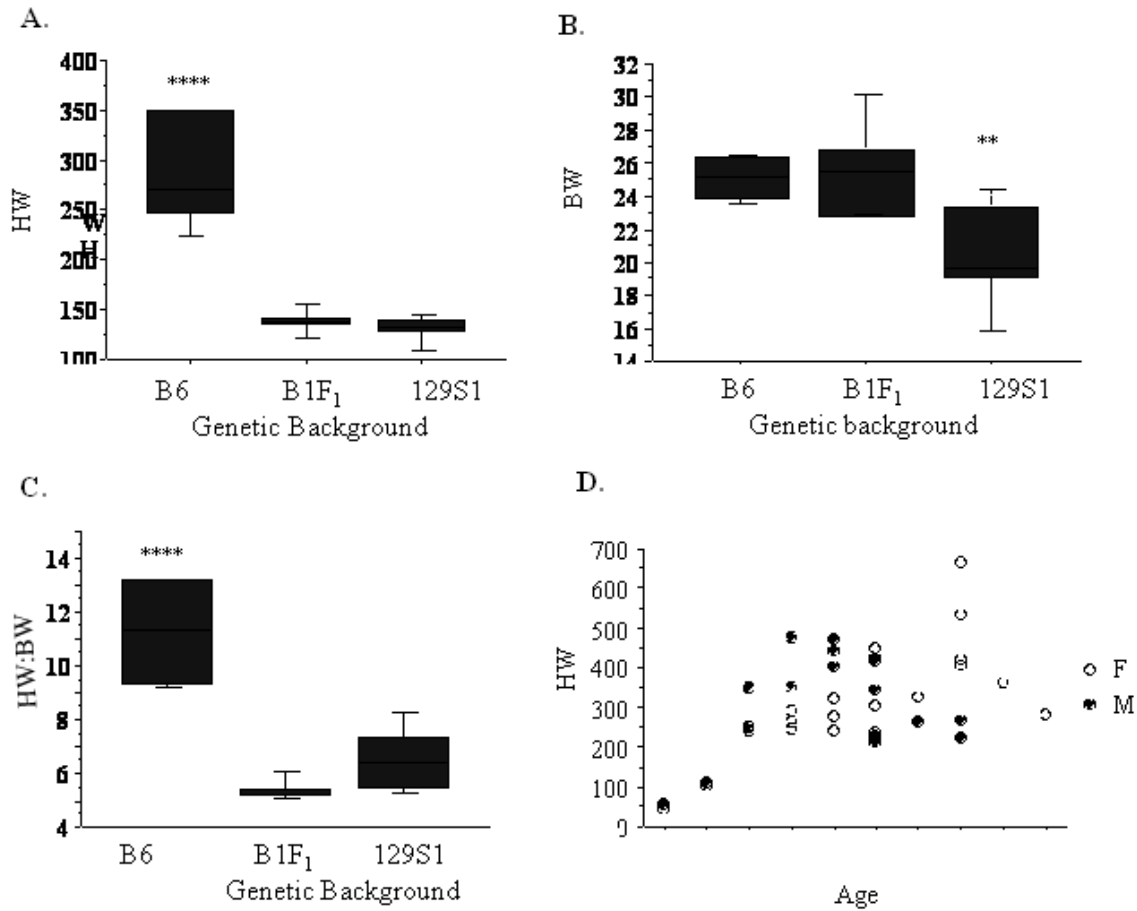
Figure 3.2: Distribution of heart weight and body weight. A) Distribution of heart weight in F2 progeny. B) Scatter plot of HW in B6, F1 (B6x129S1), 129S1 and F2 *Egfr*[wa2/wa2] mice. C) Distribution of body weight (BW) in F2 progeny. D) Scatter plot of BW in B6, F1 (B6x129S1), 129S1, and F2 *Egfr*[wa2/wa2] mice. E.) Correlation between HW and BW in F2 *Egfr*[wa2/wa2] mice. Blue arrow points to highest values from 129S1 *Egfr*[wa2/wa2] parentals and red arrow to lowest value from B6-*Egfr*[wa2/wa2] parentals.
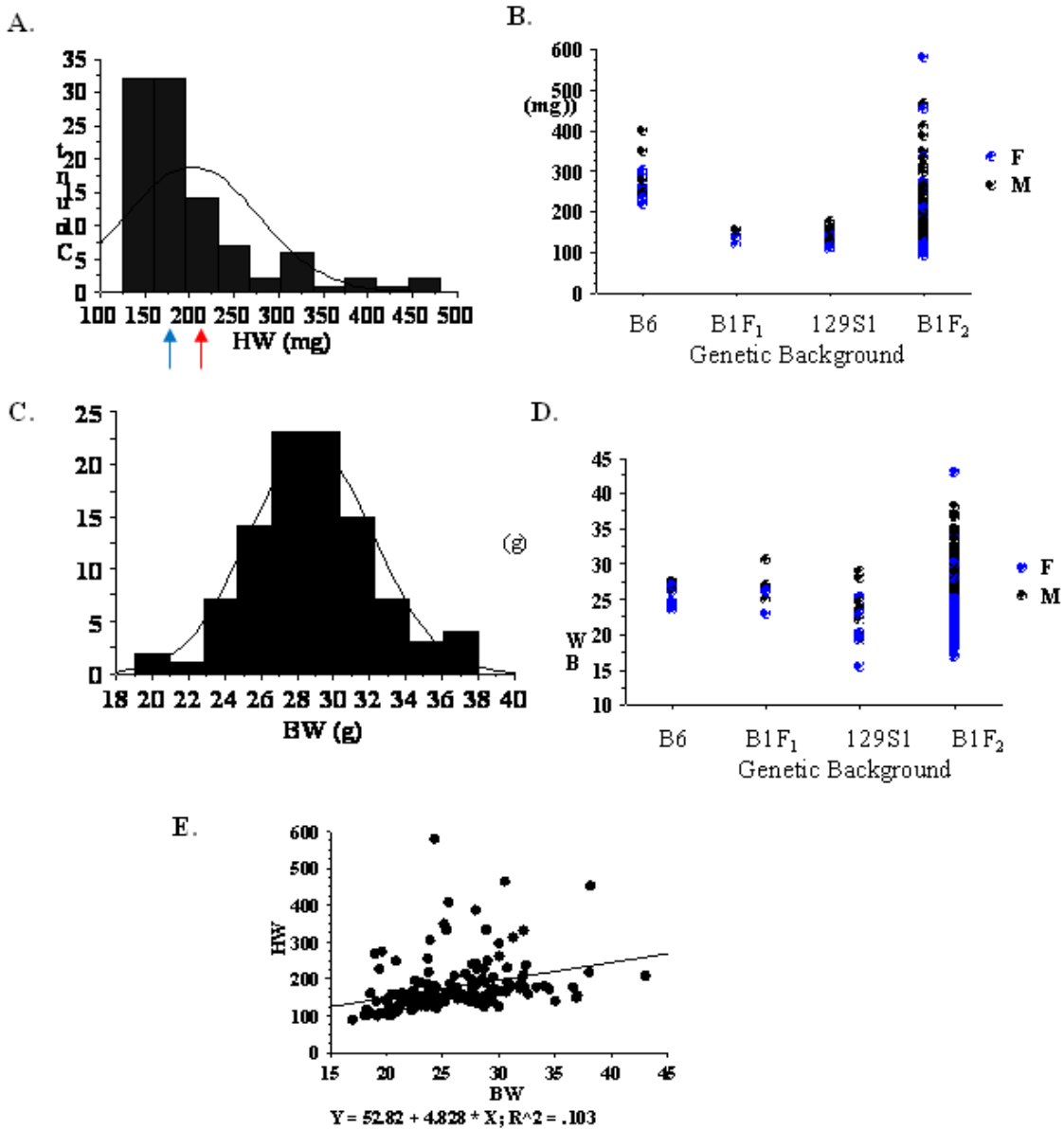
Table 3.1: Representative echocardiographic parameters and organ weights from F2 $Egfr^{wa2/wa2}$ mice

F₂ *Egfr* ^wa2/wa2^			
Mouse #	60	62	61
HW (mg)	176.9	190.1	332
H:BW (mg:g)	5.31	6.62	10.31
BW (g)	33.3	28.7	32.2
LVED, d (mm)	3.65±0.08	3.92±0.13	5.05±0.05
LVED, s (mm)	2.32±0.02	2.37±0.07	3.26±0.30
LVPW, d (mm)	0.75±0.08	1.09±0.06	0.79±0.16
LVPW, s (mm)	0.90±0.02	1.48±0.11	1.24±0.02
%FS	36.80±1.70	39.6±0.27	27.04±3.84
HR (BPM)	447±5	452±2	475±10

Figure 3.3: Representative histological sections from F2 *Egfr^{wa2/wa2}* three-month-old littermates. Arrows point to aortic (AV) and pulmonary (PV) valves. A fibrotic region (FIB) near the apex of the most severely affected heart is also indicated. Magnification = 1.6x.
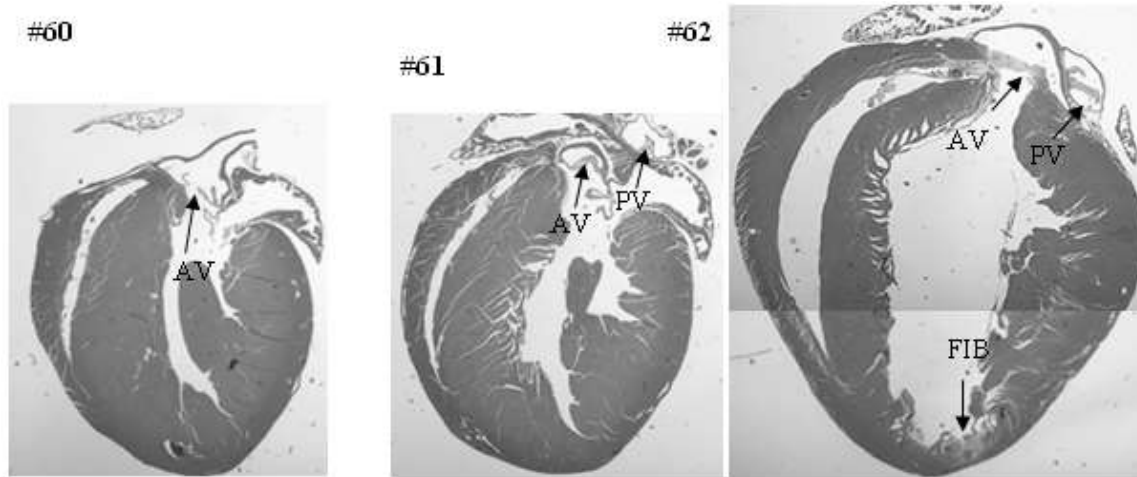
Figure 3.4: Whole genome scan performed for HW on F2 progeny, using sex as a covariate.

Two suggestive QTLs were identified.
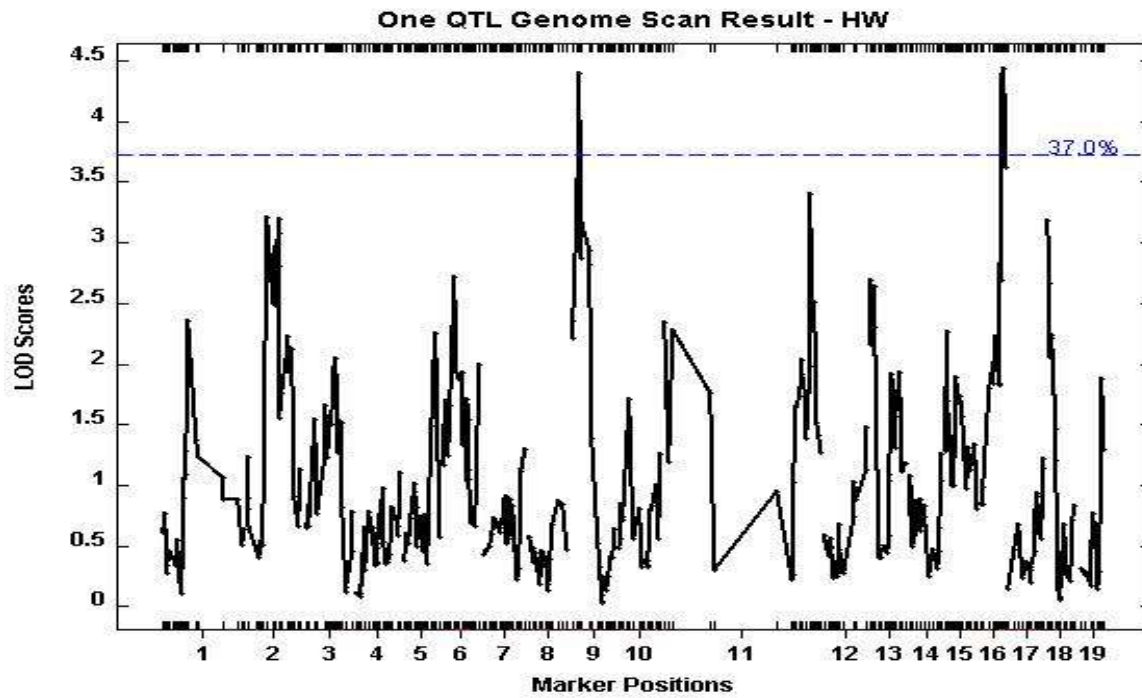
Figure 3.5: Linkage analysis on F2 male mice. A).Whole genome scan performed for HW on F2 male progeny. B) Interval mapping of the Chromosome 9 locus *Q1* in F2 male mice. C) Effect plot for marker rs13480120, which has the highest LOD.
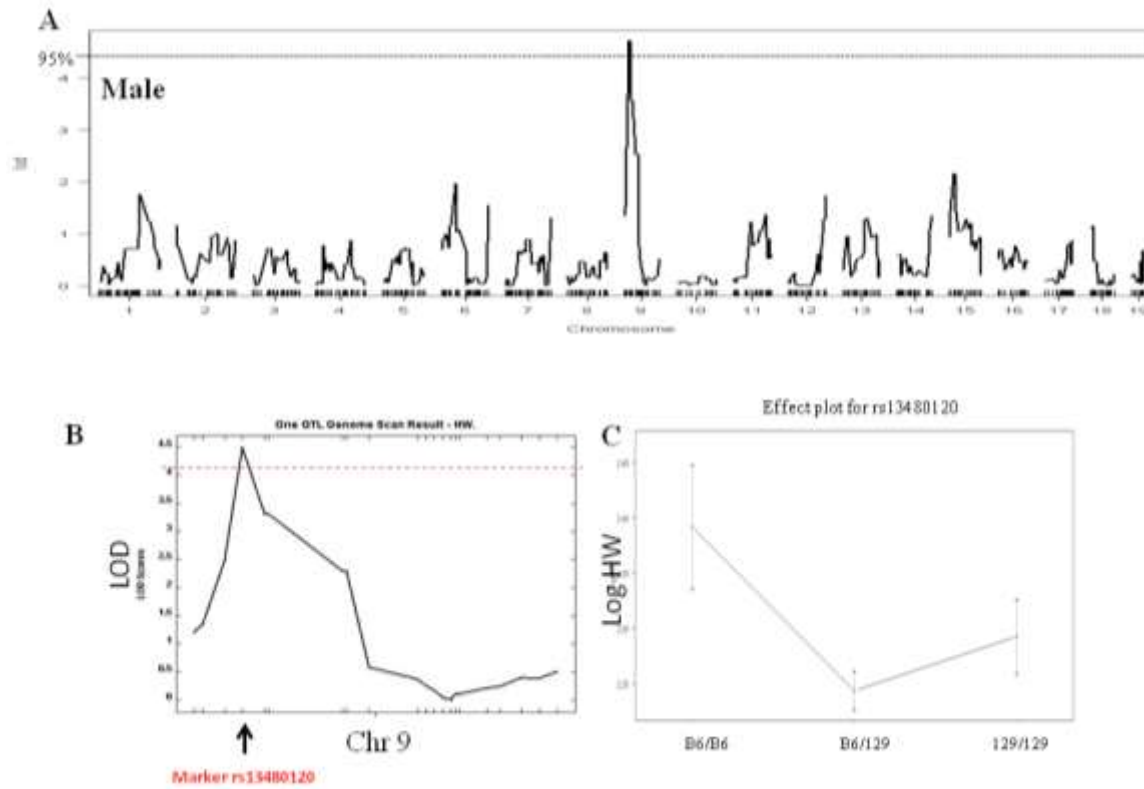
Figure 3.6 Linkage analysis on F2 female mice. A).Whole genome scan performed for HW on F2 female progeny. B) Interval mapping of the Chromosome 2 locus in F2 male mice. C) Left: interval mapping for Chromosome 2; right: effect plot for marker rs3696981, which has the highest LOD.
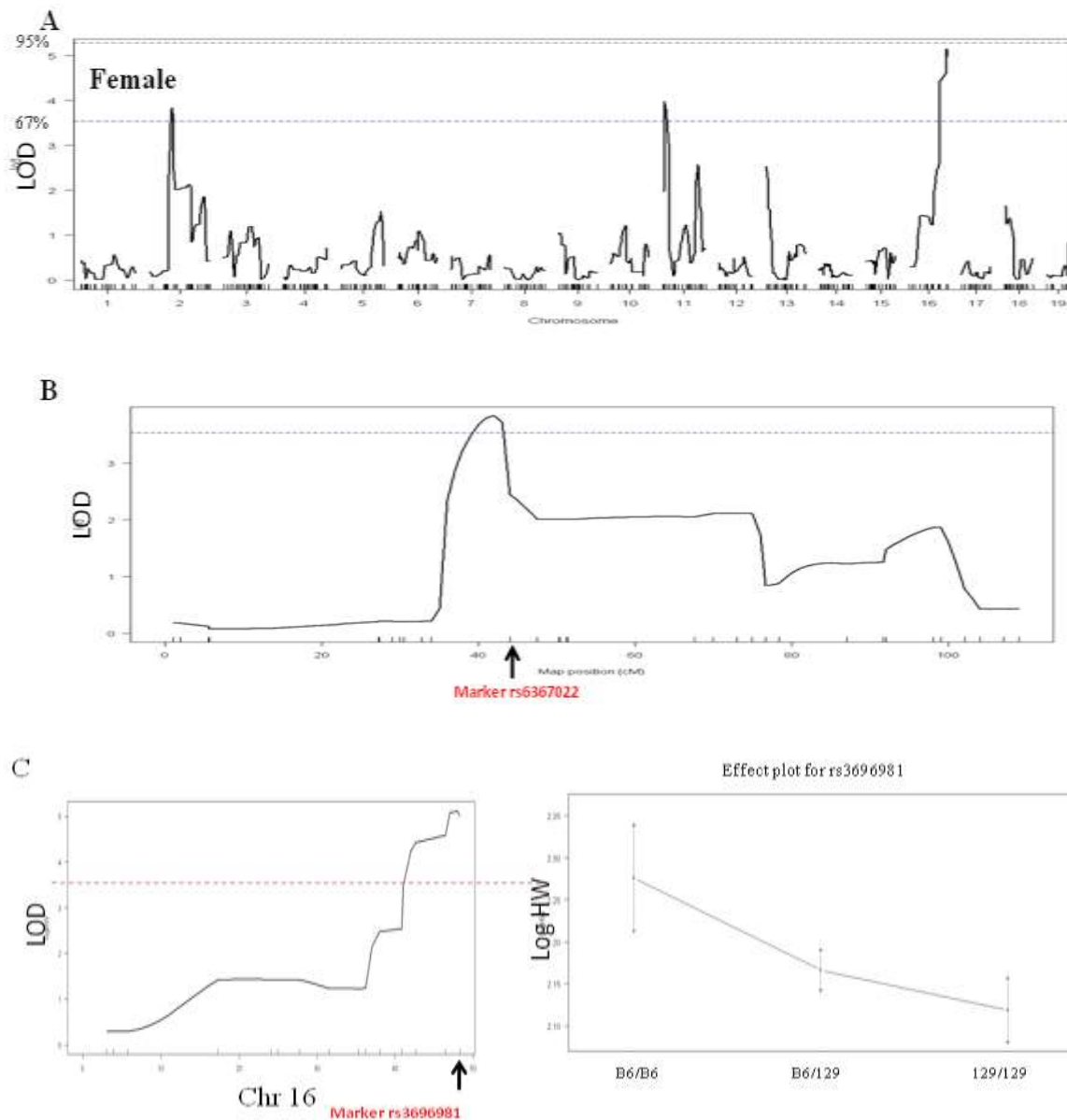
Figure 3.7: Test with increased samples size. A) Heart weight distribution among F2 male mice with B6/B6, B6/129, and 129/129 allele at *Q1* locus. B) Heart weight distribution among F2 female mice with B6/B6, B6/129, and 129/129 allele at *Q2* locus.
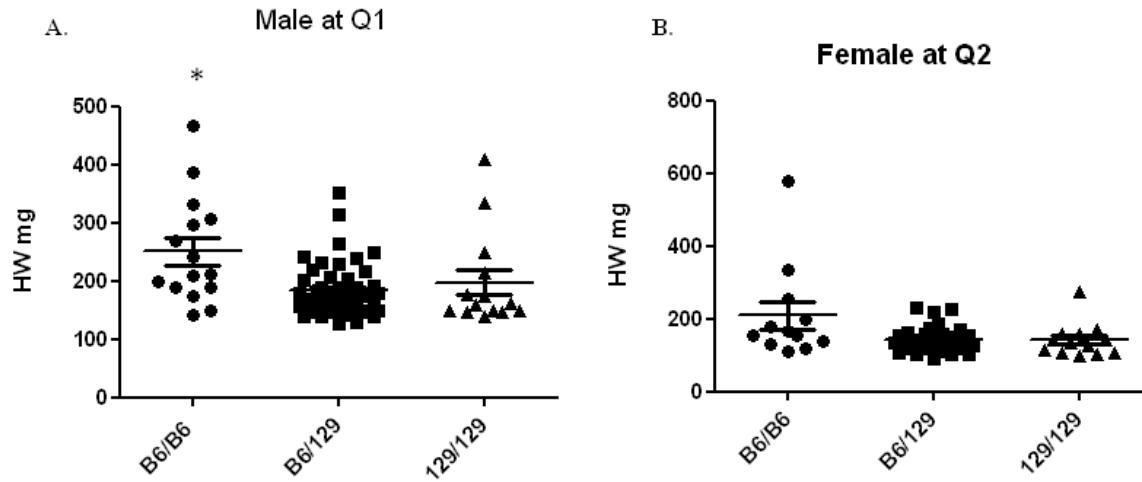
Figure 3.8: Haplotype analysis between B6 and 129/S1 at *Q1* locus

REFERENCES

1.   Hammond, I.W. et al. The prevalence and correlates of echocardiographic left ventricular hypertrophy among employed patients with uncomplicated hypertension. *J Am Coll Cardiol* **7**, 639-50 (1986).

2.   Koren, M.J., Devereux, R.B., Casale, P.N., Savage, D.D. & Laragh, J.H. Relation of left ventricular mass and geometry to morbidity and mortality in uncomplicated essential hypertension. *Ann Intern Med* **114**, 345-52 (1991).
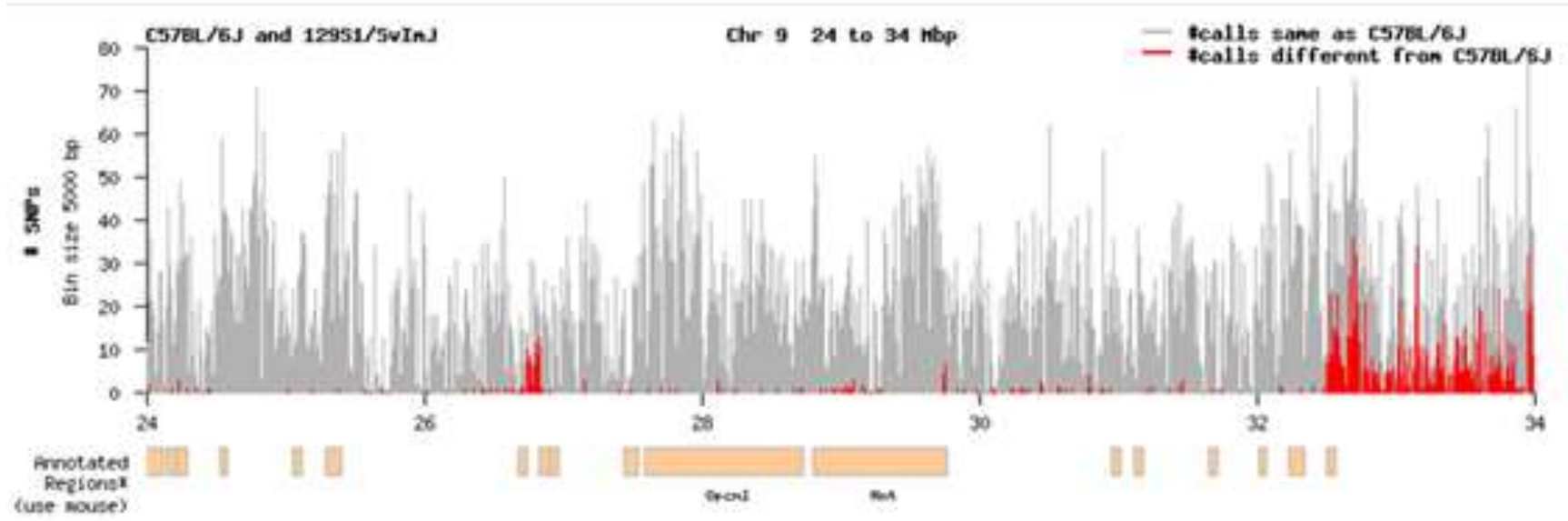
3.   Weber, K.T. & Brilla, C.G. Pathological hypertrophy and cardiac interstitium. Fibrosis and renin-angiotensin-aldosterone system. *Circulation* **83**, 1849-65 (1991).

4.   Devereux, R.B., de Simone, G., Ganau, A. & Roman, M.J. Left ventricular hypertrophy and geometric remodeling in hypertension: stimuli, functional consequences and prognostic implications. *J Hypertens Suppl* **12**, S117-27 (1994).

5.   Ganau, A. et al. Patterns of left ventricular hypertrophy and geometric remodeling in essential hypertension. *J Am Coll Cardiol* **19**, 1550-8 (1992).

6.   Levy, D., Salomon, M., D'Agostino, R.B., Belanger, A.J. & Kannel, W.B. Prognostic implications of baseline electrocardiographic features and their serial changes in subjects with left ventricular hypertrophy. *Circulation* **90**, 1786-93 (1994).

7.   Gharavi, A.G., Lipkowitz, M.S., Diamond, J.A., Jhang, J.S. & Phillips, R.A. Deletion polymorphism of the angiotensin-converting enzyme gene is independently associated with left ventricular mass and geometric remodeling in systemic hypertension. *Am J Cardiol* **77**, 1315-9 (1996).

8.   Tripodi, G. et al. Haplotype analysis of carnitine transporters and left ventricular mass in human essential hypertension. *J Ren Nutr* **15**, 2-7 (2005).

9.   Deschepper, C.F. et al. Functional alterations of the Nppa promoter are linked to cardiac ventricular hypertrophy in WKY/WKHA rat crosses. *Circ Res* **88**, 223-8 (2001).

10. Hamon, M. et al. Association of angiotensin converting enzyme and angiotensin II type 1 receptor genotypes with left ventricular function and mass in patients with angiographically normal coronary arteries. *Heart* **77**, 502-5 (1997).

11. Liljedahl, U. et al. Single nucleotide polymorphisms predict the change in left ventricular mass in response to antihypertensive treatment. *J Hypertens* **22**, 2321-8 (2004).

12. Osterop, A.P. et al. AT1 receptor A/C1166 polymorphism contributes to cardiac hypertrophy in subjects with hypertrophic cardiomyopathy. *Hypertension* **32**, 825-30 (1998).

13. Dellgren, G. et al. Angiotensin-converting enzyme gene polymorphism influences degree of left ventricular hypertrophy and its regression in patients undergoing operation for aortic stenosis. *Am J Cardiol* **84**, 909-13 (1999).

14. Orlowska-Baranowska, E. et al. Influence of ACE I/D genotypes on left ventricular hypertrophy in aortic stenosis: gender-related differences. *J Heart Valve Dis* **13**, 574-81 (2004).

15. Rockman, H.A. et al. Segregation of atrial-specific and inducible expression of an atrial natriuretic factor transgene in an in vivo murine model of cardiac hypertrophy. *Proc Natl Acad Sci U S A* **88**, 8277-81 (1991).

16. Liao, Y. et al. Echocardiographic assessment of LV hypertrophy and function in aortic-banded mice: necropsy validation. *Am J Physiol Heart Circ Physiol* **282**, H1703-8 (2002).

17. Hu, P. et al. Minimally invasive aortic banding in mice: effects of altered cardiomyocyte insulin signaling during pressure overload. *Am J Physiol Heart Circ Physiol* **285**, H1261-9 (2003).

18. Gao, X.M. et al. Regression of pressure overload-induced left ventricular hypertrophy in mice. *Am J Physiol Heart Circ Physiol* **288**, H2702-7 (2005).

19. Perrino, C. et al. Intermittent pressure overload triggers hypertrophy-independent cardiac dysfunction and vascular rarefaction. *J Clin Invest* **116**, 1547-60 (2006).

20.   Barger, P.M. & Kelly, D.P. Fatty acid utilization in the hypertrophied and failing heart: molecular regulatory mechanisms. *Am J Med Sci* **318**, 36-42 (1999).

21.   Barrick, C.J. et al. Reduced EGFR causes abnormal valvular differentiation leading to calcific aortic stenosis and left ventricular hypertrophy in C57BL/6J but not 129S1/SvImJ mice. *Am J Physiol Heart Circ Physiol* **297**, H65-75 (2009).

22.   Lygate, C.A. et al. Serial high resolution 3D-MRI after aortic banding in mice: band internalization is a source of variability in the hypertrophic response. *Basic Res Cardiol* **101**, 8-16 (2006).

23.   Li, Y.H. et al. Doppler evaluation of peripheral vascular adaptations to transverse aortic banding in mice. *Ultrasound Med Biol* **29**, 1281-9 (2003).

24.   Luetteke, N.C. et al. The mouse waved-2 phenotype results from a point mutation in the EGF receptor tyrosine kinase. *Genes Dev* **8**, 399-413 (1994).

25.   Chen, B. et al. Mice mutant for Egfr and Shp2 have defective cardiac semilunar valvulogenesis. *Nat Genet* **24**, 296-9 (2000).

26.   Broman, K.W., Wu, H., Sen, S. & Churchill, G.A. R/qtl: QTL mapping in experimental crosses. *Bioinformatics* **19**, 889-90 (2003).

27.   Manichaikul, A., Palmer, A.A., Sen, S. & Broman, K.W. Significance thresholds for quantitative trait locus mapping under selective genotyping. *Genetics* **177**, 1963-6 (2007).

28.   Skavdahl, M. et al. Estrogen receptor-beta mediates male-female differences in the development of pressure overload hypertrophy. *Am J Physiol Heart Circ Physiol* **288**, H469-76 (2005).

29.   Wiltshire, T. et al. Genome-wide single-nucleotide polymorphism analysis defines haplotype patterns in mouse. *Proc Natl Acad Sci U S A* **100**, 3380-5 (2003).

30.   Yalcin, B. et al. Unexpected complexity in the haplotypes of commonly used inbred strains of laboratory mice. *Proc Natl Acad Sci U S A* **101**, 9734-9 (2004).

Chapter IV: CONCLUSIONS AND FUTURE DIRECTIONS

EGFR belongs to the ERBB family of receptor tyrosine kinases, whose other members include ERBB2, ERBB3, and ERBB4. Upon extracellular ligand binding and receptor homo- or hetero-dimerization and activation, activated EGFR signals lead to downstream effects in cell growth, differentiation, and survival. Overexpression or mutation of EGFR contributes to a significant number of human malignancies. Thus anti-EGFR drugs have been widely used among patients with EGFR positive tumors.[1] Due to early detection and innovative therapies, cancers are now being treated as a chronic disease.[2] Although no severe cardiac side effect has been reported for EGFR targeted therapies, longer duration of anti-EGFR treatment may induce unexpected outcomes. EGFR is detectable in adult human and rodent heart. Also, human study has showed that a hypomorpic mutation in EGFR is associated with dilated cardiomyopathy in Chinese population.[3] As EGFR signaling is involved in cardiac hypertrophy through transactivation by the G protein coupled receptor (GPCR) pathway, several studies have proposed a novel treatment for hypertension and left ventricular hypertrophy, which would cause patients with cardiac dysfunction to be exposed to chronic suppression of the EGFR pathway.[4-6] Therefore, it is important to understand the role of EGFR signaling in maintaining cardiac homeostasis.

The hypomorphic $Egfr^{wa2}$ allele has been used to assess the role of EGFR signaling in normal cardiac function. Although developing cardiac hypertrophy at three months of age, $Egfr^{wa2/wa2}$ mice also develop aortic valve hyperplasia, complicating identification of the cause of

adult cardiac dysfunction.[7] Another study, using a humanized cardiomyocyte-specific dominant-negative ERBB1 to block EGFR signaling, showed that EGFR is required to prevent cardiac dilation.[8] However, because dominant-negative ERBB1 can also inactivate ERBB2 signaling through heterodimerization, this result is more likely due to the blockage of ERBB2 signaling.[8] Similarly, other studies using different systems also have the problem of off-target inhibition on ERBB2 signaling complicating the data interpretation.[9] To answer the question, we created a model with cardiomyocyte-specific deletion of *Egfr*.[10] These *Egfr* conditional mutant mice displayed a normal phenotype at young age with normal valve function. They subsequently developed progressively dilated cardiomyopathy with signs of depressed cardiac function, thinner left ventricular wall, and chamber dilations similar to *Erbb2* conditional knock-out mice. Unlike mice from *Erbb2*-CKO that develop severely dilated hearts at three-months of age, most *Egfr*-CKO mice show impaired cardiac function until six-months of age indicating that *Egfr* may be a minor pathway for maintaining cardiac function as opposed to the *Erbb2* pathway. This data is consistent with clinical results that anti-ERBB2 therapies show more conspicuous cardiotoxicity than anti-EGFR therapies in breast cancer.

The mechanism behind this dysfunction still needs to be investigated. Loss of cardiomyocytes can cause cardiac stress and dilated cardiomyopathy.[11,12] Also, over-expression of the anti-apoptotic gene Bcl-xL has shown to rescue the dilated cardiomyopathy in mice with a cardiomyocyte-restricted deletion of *Erbb2*.[10] However, TUNEL assay did not reveal significant changes in apoptosis rates between control and CKO mice at three months of age. Moreover, pathway analysis of microarray data did not show enrichment for the apoptosis pathway, consistent with TUNEL results. Furthermore, a preferential loss of homozygous *Egfr* mutant cardiomyocytes was not observed in the hearts of the adult conditional Egfr mutant mice using

qPCR for DNA from left ventricle. Thus, mechanisms other than apoptosis appear to lead to cardiomyopathy in CKO mice, such as abnormal adherens junction and impaired contractility.

It has been shown that EGFR is involved in the control of cardiac contractility activated by EGF.[13,14] Injecting an adenylyl cyclase activator can rescue the cardiac dysfunction in dominant-negative *Erbb*1 mutant mice. Therefore, impaired contractility may be the cause of cardiac dysfunction in our CKO mice.[8] Interestingly, our microarray data revealed that Integrin alpha 5 (*Itga5*) and Actin alpha 1 (*Acta1*) were the top two up-regulated genes. Integrins mechanically link the extracellular matrix to the internal cytoskeleton and in hear and thereby involved in mechanotransduction. Also, integrin is showed to up-regulated in the heart with pressure overload indicating a potential role for integrins in the hypertrophic response.[15] Previous study has shown that enhanced *Itga5* signaling in adult heart, in absence of pressure overload, leads to marked conduction abnormalities, contractile dysfunction and sudden death.[16] α-cardiac actin and skeletal α-actin (*Acta1*) are two isoforms co-expressed in normal adult myocardium.[17] Studies have shown that *Acta1* gene expression is up-regulated in the human hearts with left ventricular hypertrophy or valvular diseases.[18] Also, cardiac contractile function appears to correlate with the content of Acta1 in cardiomyocytes. Recent study has shown that SH2-containing protein tyrosine phosphatase 2 (SHP2), an EGFR downstream effector, negatively regulate Acta1 gene expression.[11] All these results indicate that impaired contractility may be the cause of dilated cardiomyopathy in our CKO mice. Future goals will unravel the potential effects of EGFR on cardiac contractility through assessing maximal isometric force production under conditions of comparable preload in left ventricle, sarcomeric shortening and Ca^{2+} transients in isolated cardiac myocytes, and electrical propagation. We hope that by

identifying the mechanism causing dilated cardiomyopathy in CKO studies will help in managing or reducing the long-term cardiac toxicity in patients with EGFR-targeted therapies.

Erbb2 targeted mono-therapy, Trastuzumab, has revealed a low incidence of cardiac dysfunction (1%) in patients.[19] However, the incidence of cardiac side effects of a Trastuzumab mono-therapy is found to increase to 7% in patients with previous exposure to anthracyclines, which are known cardiotoxic agents. Also, when Trastuzumab therapy is combined with anthracyclines, cardiac side effect is augmented to 27%.[19] EGFR targeted therapies are frequently administered on top of standard chemo-therapies, which emphasizes the importance of knowing the possible role of EGFR pathway in cardioprotective responses. Moreover, because EGFR signaling is indispensable to develop cardiac hypertrophy induced by GPCR pathway, people have proposed a novel treatment to prevent left ventricular hypertrophy using EGFR inhibitors. To determine the role of EGFR in heart with pressure overload, aortic-banding was carried out in both control and *Egfr* CKO mice. CKO mice showed a significant decrease of fractional shortening (FS%) compared with wild-type controls. Also a subset of CKO mice developed dilated cardiamyopathy, an end-stage of cardiomyopathy, two weeks post surgery, but none of the wild-type mice showed dilated heart. This result indicated that EGFR-dependent pathways are indispensable to withstand cardiac injury imposed by pressure overload. With our CKO mice, we can also test the cardiotoxicity using different therapy combinations, such as anthracycline and doxorubicin, which are commonly used anti-cancer drugs. Characterization of cardiac phenotypes of our CKO mice in response to different treatment combinations would be helpful to increase therapy efficiency and reduce cardiac-toxicity in patients under chronic EGFR-target therapies.

Genetic variation has an important role in patients' response to ERBB targeted therapies.[20,21] As shown above, only 1% of patients with breast cancer under ERBB2 targeted mono-therapy have cardiac dysfunction. Also, the high accumulation of Gefitinib, an anti-EGFR drug, was shown to associate with heterozygosity for the 421C→A allele at the *ABCG2* locus compared with homozygous controls. In addition, this high accumulation would likely be relevant to toxicity and therapeutic effects.[20] Also, mice homozygous for a hypomorphic mutation in the *Egfr* (*Egfr^{wa2}*) have shown a background dependent variation of resulting phenotypes, which mimic the toxicities observed in patients with EGFR targeted therapy. Using these mice models with 55 mice, we mapped one QTL locus (*Edlvh1*) for left ventricular hypertrophy on Chr 9 that contains thirteen candidate genes and another putative QTL locus (*Edlvh2*) for female mice on Chr16. *Edlvhq1*, a 129S1 dominant locus, identified in our mapping panel is a moderate contributor to the heart weight with great potential to be a clinically relevant modifier in human studies.

Haplotype analysis comparing B6 and 129S1 genomes narrowed the candidate region for *Edlvh1* and revealed that several cardiac function related genes, such as *Kcnj1* and *Ets1*, are located in this candidate region. Protein encoded by *KCNJ1* is an integral membrane protein and potassium channel. Polymorphisms in the *KCNJ1* gene showed associations with blood pressure and left ventricular mass in human, which makes it a potential candidate. To assess the candidate genes at the *Edlvh1* locus, allele specific PCR can be performed to identify possible differential expression from B6 versus 129S1 alleles in F1 *Egfr^{wa2/wa2}* mice.

Edlvh2 for female, located on Chr16, was also highlighted in our study. This locus was not significant after expanding our sample size. However, two female outliers all have homozygous B6 allele in *Edlvh2* locus and another suggestive QTL locus on Chr2, indicating

possible gene-gene interactions in female mice. We are adding 89 new samples to our interval

mapping, and would expect to confirm previous QTLs and also identify more QTLs.

Successful identification of genetic modifiers for cardiac dysfunctions in low EGFR

activity model would increase our knowledge about the role of EGFR in normal heart function,

and may assist prediction of cardiac toxicity in sensitive population.

REFERENCES

1.   Chen, M.H., Kerkela, R. & Force, T. Mechanisms of cardiac dysfunction associated with tyrosine kinase inhibitor cancer therapeutics. *Circulation* **118**, 84-95 (2008).

2.   Force, T., Krause, D.S. & Van Etten, R.A. Molecular mechanisms of cardiotoxicity of tyrosine kinase inhibition. *Nat Rev Cancer* **7**, 332-44 (2007).

3.   Zhou, B., Rao, L., Peng, Y., Zhang, Q. & Zhang, L. Epidermal growth factor receptor gene polymorphisms, R497K, but not (CA)n repeat, is associated with dilated cardiomyopathy. *Clin Chim Acta* **403**, 184-7 (2009).

4.   Asakura, M. et al. Cardiac hypertrophy is inhibited by antagonism of ADAM12 processing of HB-EGF: metalloproteinase inhibitors as a new therapy. *Nat Med* **8**, 35-40 (2002).

5.   Shah, B.H. & Catt, K.J. Matrix metalloproteinase-dependent EGF receptor activation in hypertension and left ventricular hypertrophy. *Trends Endocrinol Metab* **15**, 241-3 (2004).

6.   Smith, N.J., Chan, H.W., Osborne, J.E., Thomas, W.G. & Hannan, R.D. Hijacking epidermal growth factor receptors by angiotensin II: new possibilities for understanding and treating cardiac hypertrophy. *Cell Mol Life Sci* **61**, 2695-703 (2004).

7.   Chen, B. et al. Mice mutant for Egfr and Shp2 have defective cardiac semilunar valvulogenesis. *Nat Genet* **24**, 296-9 (2000).

8.   Rajagopalan, V., Zucker, I.H., Jones, J.A., Carlson, M. & Ma, Y.J. Cardiac ErbB-1/ErbB-2 mutant expression in young adult mice leads to cardiac dysfunction. *Am J Physiol Heart Circ Physiol* **295**, H543-54 (2008).

9.   Barrick, C.J., Yu, M., Chao, H.H. & Threadgill, D.W. Chronic pharmacologic inhibition of EGFR leads to cardiac dysfunction in C57BL/6J mice. *Toxicol Appl Pharmacol* **228**, 315-25 (2008).

10.   Crone, S.A. et al. ErbB2 is essential in the prevention of dilated cardiomyopathy. *Nat Med* **8**, 459-65 (2002).

11.   Nakaoka, Y. et al. SHP2 mediates gp130-dependent cardiomyocyte hypertrophy via negative regulation of skeletal alpha-actin gene. *J Mol Cell Cardiol* **49**, 157-64.

12.   Chien, K.R. Stress pathways and heart failure. *Cell* **98**, 555-8 (1999).

13.   Pareja, M., Sanchez, O., Lorita, J., Soley, M. & Ramirez, I. Activated epidermal growth factor receptor (ErbB1) protects the heart against stress-induced injury in mice. *Am J Physiol Regul Integr Comp Physiol* **285**, R455-62 (2003).

14.   Nair, B.G., Rashed, H.M. & Patel, T.B. Epidermal growth factor produces inotropic and chronotropic effects in rat hearts by increasing cyclic AMP accumulation. *Growth Factors* **8**, 41-8 (1993).

15.   Babbitt, C.J., Shai, S.Y., Harpf, A.E., Pham, C.G. & Ross, R.S. Modulation of integrins and integrin signaling molecules in the pressure-loaded murine ventricle. *Histochem Cell Biol* **118**, 431-9 (2002).

16.   Valencik, M.L. et al. Integrin activation in the heart: a link between electrical and contractile dysfunction? *Circ Res* **99**, 1403-10 (2006).

17.   Vandekerckhove, J., Bugaisky, G. & Buckingham, M. Simultaneous expression of skeletal muscle and heart actin proteins in various striated muscle tissues and cells. A quantitative determination of the two actin isoforms. *J Biol Chem* **261**, 1838-43 (1986).

18.   Suurmeijer, A.J. et al. Alpha-actin isoform distribution in normal and failing human heart: a morphological, morphometric, and biochemical study. *J Pathol* **199**, 387-97 (2003).

19.   Sparano, J.A. Cardiac toxicity of trastuzumab (Herceptin): implications for the design of adjuvant trials. *Semin Oncol* **28**, 20-7 (2001).

20.   Li, J. et al. Association of variant ABCG2 and the pharmacokinetics of epidermal growth factor receptor tyrosine kinase inhibitors in cancer patients. *Cancer Biol Ther* **6**, 432-8 (2007).

21.   Liu, X. et al. Neuregulin-1/erbB-activation improves cardiac function and survival in models of ischemic, dilated, and viral cardiomyopathy. *J Am Coll Cardiol* **48**, 1438-47 (2006).